PROGRESS REPORT NO. 20-195

THE LIQUID-PHASE MIXING
OF A PAIR OF IMPINGING STREAMS

JACK H. RUPE

Jet PROPULSION LABORATORY

CALIFORNIA INSTITUTE OF TECHNOLOGY

PASADENA 3, CALIFORNIA

AUGUST 6, 1953

Progress Report No. 20-195

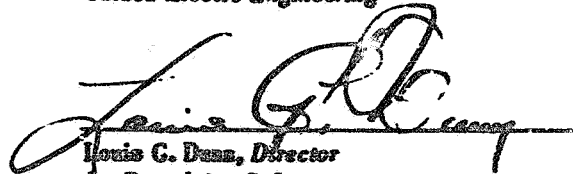# THE LIQUID-PHASE MIXING OF A PAIR OF IMPINGING STREAMS

Jack H. Rupe

Robert F. Rose, *Chief*
Propulsion Section

Jack E. Froehlich, *Chief*
Guided Missile Engineering

Louis G. Dunn, *Director*
Jet Propulsion Laboratory

Copy No._____

73

TABLE OF CONTENTS

LIST OF TABLES

LIST OF FIGURES

LIST OF FIGURES (Cont'd)

ABSTRACT

*The simultaneous distribution of two liquids in the spray resulting from the impingement of
a pair of liquid streams has been determined experimentally. The relative effectiveness of the mixing
process was evaluated by a mixing factor that is dependent on the variation in local mixture ratio.
The correlation of this mixing factor with injector parameters shows the relative importance of
stream momenta and effective impingement area on the spray configuration. The application of the
data to rocket injector design is outlined.*

I.   INTRODUCTION

The operation of a rocket motor is dependent on the chemical reaction of a propellant or
propellant combination to liberate heat and energy that may in turn be utilized to produce thrust. The
basic tenets thus stipulated are not difficult to attain under conditions where the time available for
reaction is very long, the degree of utilization of the available energy is unimportant, and the
efficiency of the reaction can be ignored. However, many practical complications arise when it
becomes necessary to optimize the performance of a device that is intended to transform energy
at one at tremendous rates in an orderly and controlled manner so as to produce consistently pre-
dictable results.

Most of these complications are due to restrictions (1) on the physical size of a combustion
chamber with consequent limitations in gas residence time and/or reaction time and (2), in the case
of liquid-propellant motors, on prereaction phenomena. Therefore, for the case of the monopropellant
system, primary emphasis must be placed on heat transferred from the reacting gases to continuously
injected liquids. It is certain that a minimum quantity of heat transfer is required in order to sustain
the reaction of an otherwise stable compound. Since this energy is not actually lost in the over-all
system, it is reasonable to conclude that heat transferred in addition to the minimum requirement
will accelerate reaction rates, thereby increasing energy release for a given chamber volume and
hence tending to optimize the over-all configuration. Thus it would appear possible to approach an
optimum monopropellant injection system by increasing the heat transfer from gas to liquid by all
possible methods, for instance, by increasing propellant atomization and producing a uniform mass
distribution across the injection surface.

In biliquid systems, as for the monopropellant case, it must be assumed that the heat transfer
from the gas to the liquid is an important prereaction requirement and that an optimum configuration
can be approached in a similar manner. This requirement must be particularly important for those
propellants that are nonhypergolic at normal injection temperatures since they require (as does a
monopropellant) a certain minimum quantity of heat transfer in order to initiate the reaction. For

hypergolic propellants this minimum heat transfer can be somewhat less since it is necessary to supply only enough heat to the injected liquids to prevent quenching by the unmixed propellants. In any case, an optimum value will undoubtedly be approached for the condition of maximum heat transfer; if it is assumed that the energy feedback is in direct proportion to the total energy released, it makes no difference whether the mechanism be radiation, conduction, convection, or wave propagation so long as the ultimate reaction is optimized.

Biliquid rocket systems introduce additional complications since they require a configuration that will produce a certain degree of mixing of the propellants prior to reaction and within the confines of the combustion chamber (Cf. Ref. 1). The actual mixing may take place in a number of different ways: it will, in most conceivable cases, be the cumulative result of the processes of liquid-phase mixing, vaporization, diffusion, and gaseous turbulence due to the expansion of combustion. The physical differences in most injector designs might be traced to the fact that primary emphasis is placed on one of these contributing factors. However, in an optimum configuration it is required that each contributing factor be utilized to the limit where overemphasis actually degrades the over-all mixing process. Behind this last statement lies the implicit assumption that an optimum reaction predicates intimate physical mixing on a molecular scale and in the proper proportions for a stoichiometric and/or optimum reaction. In the ideal case this condition would exist immediately after injection and prior to reaction; the reaction time (or more appropriately the mixing time) would approach a minimum, and combustion volume could be reduced to a minimum (or optimum) size. By thus defining the prerequisites of an optimum reaction, the primary function of a biliquid rocket-motor injector has been stated, at least in part.

Evaluation of the mixing process as performed by a biliquid injector must stem from consideration of the spatial distribution attained simultaneously by two liquids as well as of the scale and size of the controlling particle. Strictly from the standpoint of the injector, the spatial-distribution configuration has very little significance since it can be assumed that, if necessary for the production of an optimum motor, it would be possible to construct a combustion chamber having any required geometry. On the practical side, however, it would be convenient to be able to control the spatial distribution so as to optimize injection into the more convenient combustion-chamber shapes. Thus for optimum injection it is required only that the spatial distribution of the two liquids be identical so as to provide each unit space of the prereaction region with a predetermined optimum mixture ratio.

The optimum scale of mixing undoubtedly occurs on a molecular basis, both for liquid and for gaseous states, but it is doubtful that such a fine scale of mixing is ever attained in any real case prior to combustion. Rather, it might be visualized that macro-scale mixing consisting of a dual distribution of discrete particles in the liquid phase is followed in time by selective vaporization of one component to produce one liquid propellant dispersed in the gas phase of the second component and then ultimately by the two propellants being further mixed, dispersed, and reacted in the gas phase. Though the complications of the reaction process, subsequent gas turbulence, heat transfer, etc. are

many and varied, they cannot alter the basic concept of the over-all process.

The configuration just described might be attained by separate injection of two liquids into the same region, but it is inconceivable that the uniformity or scale of mixing thus attained could ever exceed that which should be possible by mixing in the liquid phase prior to distributing the liquids (in a similar and equally efficient manner) to the combustion zone. The scale of mixing thus attained should prevail throughout the prereaction zone and thereby complement the processes of evaporation, diffusion, and turbulence.

The possibility that the liquids might be immiscible suggests that the dual distribution just referred to might actually be attained. On the other hand, it is more likely that a fairly fine emulsion would be formed if the energy available were properly utilized. Even though the mixture thus formed was not stable enough to be classed as a true emulsion, it is doubtful that any deleterious effects could be observed because of the very short lifetimes required. If it is then assumed that such dispersions could be formed, it could be expected (Cf. Ref. 2), that the emulsion scale would be small relative to particle size (of the order of 0.2 to 50 microns as compared with some 200 to 400 microns as the approximate mean diameter of an impinging stream spray) and that subsequent processes of reaction and evaporation follow essentially the same pattern as that taken by miscible liquids. It is interesting to note the possibility of increasing the emulsification and hence liquid-phase mixing of immiscible liquids by the simple expedient of adding a suitable wetting agent.

Qualitative experimental evidence has shown that the degree of mixing attained with biliquid injectors has a considerable effect upon rocket-motor performance (Cf. Refs. 3 and 4). A similar conclusion results from any logical analysis of the requirements for optimum reaction. The reasoning of this discussion and the assumption that the prereaction mixing could contribute the major portion of the over-all process led to an investigation which was concerned with the evaluation of liquid-phase mixing and the determination of the influence of the controlling parameters.

The physical arrangement of the various injection schemes that have been utilized for rocket-motor injection has near-infinite variety, but in almost all cases the basic element is a more or less simple orifice. In biliquid injection one of the most popular schemes for obtaining mixing and for controlling distribution consists of two or more streams impinging at a common point. The relative simplicity in design and construction of such injectors, together with positive control of propellant mass-flow rate, accounts for the general acceptance of this basic design. The probability that information on impinging-stream injectors would benefit a majority of interested people and the necessity for some restriction on the scope of the experimental program resulted in this investigation of the liquid-phase mixing of a single pair of impinging streams.

II.   ANALYSIS OF PROBLEM

A direct determination of the liquid-phase mixing attained by actual propellant combinations might be possible if steps were taken to prevent a reaction. However, the ever-present possibility of explosion, together with the difficulty in handling liquids such as nitric acid and liquid oxygen, suggests the alternative of simulating propellants with more suitable liquids and extending the investigation to include the effects of the physical properties of liquids. This method also has the advantage of increasing flexibility and scope of data obtained. It is possible that data related to liquid-phase mixing could be obtained by sampling and analyzing the reaction products in a motor chamber, but at best this procedure would result in an indirect correlation.

Experimental determination of the spray characteristics that may be used to evaluate liquid-phase mixing, i.e., variation in local mixture ratio and the variation in mass distribution within the spray, may best be accomplished by some direct sampling technique. In order to keep the sampling area small relative to the spray cross section, such methods always imply the necessity for discrete sampling at a great number of points with the associated cumbersome quantities of data to be reduced. Unfortunately there can be no experimental alternative until it has been proved that simpler methods are applicable.

The sample itself can be made to measure the variation in mass distribution within the spray by controlling sampling time, but it is also necessary to devise a method of determining the mass ratio of one liquid to the other. The use of liquids of different physical properties presents a great number of possibilities, but the two simplest schemes involved the use of (1) immiscible liquids of different densities and (2) the same liquid or miscible liquids for both streams but with one component dyed. Direct measurement of two volumes provides the necessary information in the first method, and a calibrated photometer provides the required numbers in the second system. Although both techniques were used, the first method was chosen for most of these tests since it was considerably faster and allowed the near duplication of the physical properties of the acid-aniline propellant system with the substitution of carbon tetrachloride and water as the sprayed liquids. It is interesting to note that nitric acid and aniline are also believed to be immiscible. As mentioned in Section I, the immiscibility of the sprayed liquids should not affect the results obtained as long as the local sampling area is made large relative to spray particle size; for most practical arrangements this condition is unavoidable.

When a simulation method is used, some consideration must be given to the possible effects of a reaction that would in actual practice be sustained at a point near the stream impingement. The actual location and stability of the so-called reaction front and the influence and/or necessity of vaporization and heat transfer are still unknown, but several factors can be considered. First, it is certain that a biliquid reaction cannot occur until some mixing has taken place. Second, the spray formed by a pair of impinging streams consists of particles traveling radially from a near point

source at the impingement point. Since the rate of increase of the spray volume with distance is quite high (with a subsequent decrease in liquid concentration p.. unit of spray volume), the probability of secondary collision beyond the impingement point becomes quite low. Third, the probability of secondary collisions of particles in the proper proportion for efficient combustion must be very small. Thus it would appear that such liquid-phase mixing as is obtained must be completed within a very short distance (and therefore short time interval) from the point of impingement. Even though the liquids are hypergolic and the chamber temperature, pressure, and heat transfer are quite high, it is conceivable that these effects on the initial mixing process are quite small. Therefore, if by experiment it is possible to determine an effect on liquid-phase mixing of nonreacting liquids with varying dynamic characteristics of the free streams, it is reasonable to assume that similar effects must occur in a rocket motor. This premise is, in fact, the basis for the experimental study herein described.

Aside from the physical properties of the sprayed liquids, the choice of parameters to be investigated was the result of an elementary analysis of the dynamics involved in the impingement of liquid streams. The geometry of the system was defined as shown in Figure 1. Thus the computed resultant momentum line was taken as the spray center line and coincided with the vertical center line of the spray-sampling device. Hence the horizontal component of momentum of each of the two streams was always set equal. Consideration of such a system led to the hypothesis of several requirements for optimum mixing that may be summarized as follows:

1. The specific surface of impact, i.e., impingement surface area per unit mass rate of liquids, must approach a maximum in order to attain maximum conversion of the convergent energy vector into turbulence and mixing. For the case of impinging streams of circular cross section with which this study is concerned, it is required that the stream diameters be equal;* that is,
$$A_1/A_2 = (D_1/D_2)^2 = 1.0.$$

2. In case two small particles, one from each stream traveling a collision course, are followed through the point of impact, it is seen that the ideal situation would exist when an inelastic collision occurred to form a single particle of optimum mixture ratio and if the particle were to leave the impact surface so as to produce a minimum disturbance to adjacent particles. It is readily seen that this condition is attained only when the moments of the two particles are equal, i.e., when the resultant path of the particles follows the line of the bisection of the stream center line. Under any other condition the high momentum stream will cause excessive reflection of the low momentum stream with subsequent "splitting" or "rolling over" of the low momen-

---

*The nomenclature used in this report is given in Table I.

turn stream, thus preventing proper mixing. Hence $M_1/M_2 \approx 1.0$ is an optimum condition.

3. In the original hypothesis it was reasoned that the impact-induced turbulence (and therefore the turbulent mixing) should increase and approach a maximum as the impingement angle increased from zero and approached $180°$. However, experimental data indicated that a parameter akin to contact time had considerable influence and was also proportional to the impingement angle. Thus the over-all effect was not as simple as supposed (Cf. Section VIII). Therefore impingement angle in itself must be considered important from a mixing standpoint in addition to its marked effect on spatial distribution.

4. Even though each of the first three criteria is fixed at some optimum value, it is conceivable that the varying of stream velocity may influence somewhat the degree of mixing attained. (This condition is possible if it is assumed that choice of propellant combinations allows variation in liquid density and mass rates in an otherwise fixed configuration.) Assuming that some sort of interface exists, the velocity differential would create turbulent eddies to promote the mixing of the two liquids. However, the scale and magnitude of such turbulence may be negligibly small compared with initial stream turbulence and that produced at impact. On the other hand, it is reasonable to assume that the kinetic energy available in the form of turbulence and for the production of turbulence at such an interface may influence the over-all mixing. Thus the energy level of the streams as well as energy available for mixing may be influential parameters.

5. Of more cursory interest were the dimensional quantities of impingement length and orifice area. Except as orifice area might influence Reynolds number and therefore stream turbulence and as impingement length might be affected by fabrication tolerances and jet directional stability, there was no basis for expecting these factors in themselves to have any influence in mixing.

These several parameters were considered most important and were investigated experimentally to determine their effect on liquid-phase mixing. Because of the near-infinite number of physical arrangements of injector components that are feasible, a pair of streams of circular cross section was used to obtain the bulk of the data. However, there is evidence to indicate that trends established for circular streams are directly applicable to other stream cross sections and that it may be possible to extend general conclusions to combinations of three or more orifices.

III. APPARATUS

The equipment used for this investigation consisted of three basic components, i.e., an impinging jet assembly, a spray collector, and a spray booth with its associated spray shutter, controls, and photographic installations.

The impinging-jet assembly as shown in Figure 2 was constructed to provide means of varying the impingement angle and impingement length (or distance), controlling the resultant momentum line of the spray, and allowing installation of various orifice pairs in a nearly identical installation. The barrels for mounting the various orifices were designed for the maximum practical contraction ratio in an attempt to minimize the influence of flow conditions upstream from the orifice. Provisions were also made for the installation of baffles and screens to obtain additional turbulence damping. The orifice mounting is a screw-insert type using metal-to-metal seal so that within fabrication tolerances the orifice entry plane coincides with the internal surface of the barrel.

The impingement angle was controlled by driving the individual barrels along a fixed quadrant with a rack and pinion. The barrels were locked in their mounting blocks with lock nuts which provided both the adjustment for impingement length and the necessary adjustment for stream alignment. This arrangement also allowed the rotation of one complete orifice-barrel assembly (and therefore stream) relative to the other stream. Pressure measurements were made within the barrel but upstream from the last turbulence-damping screen, thus providing suitable information since the screen produced a negligible pressure drop even with maximum flow through the largest orifices investigated. The details of this barrel assembly as used to obtain the bulk of the data are shown in Figure 3.

Four collectors were designed for use in determining the spatial distribution and in evaluating the local mixture ratios within a spray. The only differences between the collectors were in size and arrangement; thus provision was made to obtain samples within the same spherical segment but at different radial distances, i.e., 2, 3, 4, and 6 inches. The object, of course, was to determine any possible effects due to sampling distance. However, it was believed that this information must have little significance for any system wherein the spray particles emanate from a near point source. Since fabrication costs were fairly high, only one collector of the set was constructed. Two views of this collector used for obtaining samples on the spherical surface having a 6-inch radius are shown in Figure 4.

The assembly consists of four radial banks of tubes equally spaced around the spray axis intercepting a maximum cone angle of 100°. The tubes are made from precision-bore glass tubing having an inside diameter of 0.1700 ± 0.0002 inch and are positioned 0.250 inch center to center. For purposes of identification, each radial arm was assigned a letter, i.e., A, B, C, or D; and each tube was given a number starting with 1 for the tube next to the center tube and continuing in succession to the outermost tube. The center tube was given the identification zero. The metal

tubes located on the sampling-surface tips have entrance angles adjusted to intercept that portion of an ideal spray included in a segment having a base area equal to the cross-sectional area of the vertical tubes. An ideal spray in this case refers to a spray in which all the particles travel radially from a point source. In most configurations this condition may be assumed since the effects of extraneous air currents and gravity may be considered to be negligible. One end of each tube is sealed at a common reference plane; thus the height of the column collected per unit time interval is directly proportional to the local mass rate at the sampling surface. Since the collector was constructed in three pieces (Cf. Fig. 4), two photographs of each sample provide the histograms of the spatial distribution attained on four radii about the spray axis. By taking additional samples with different relative collector positions, a complete survey of a spray cross section may be obtained. Furthermore, if two immiscible liquids are used as the sprayed liquids, or if provision is made to evaluate some common property of miscible liquids, such samples provide the information required for the determination of the variation in local mixture ratios attained in a biliquid system. A typical series of samples obtained with carbon tetrachloride and water for six different collector positions is presented in Figure 5.

The spray booth shown in Figure 6 provides a reasonably quiescent chamber within which the collector may be exposed to the spray for a controlled time interval. An exhaust system maintains a continuous downdraft within the booth so as to minimize the toxic dangers involved in spraying such liquids as CCl_4. This system also aids in maintaining a relatively mist-free field when sprays are photographed. The air velocities within the booth are of the order of 0.3 ft/sec and therefore have a negligible effect on spray configurations.

The collector exposure time is determined by the controlled speed of a rotating slot that is driven by a constant-speed motor through a variable-speed transmission. The slot itself is an annulus bounded by two radial lines and is cut into a disk that is perpendicular to the spray axis and intercepts the spray approximately 0.5 inch below the impingement point. The edge of the slot contains provision for diverting liquid into the drain trough in order to provide sharp spray cutoff and minimize dripping of liquid from the disk surface. Exposure times down to about 0.5 second are obtained by manual control of the drive-motor switch. (Note that this procedure does not define the accuracy of exposure times since the shutter accelerates to full speed in about a quarter revolution). Although the data reported herein were obtained with manual shutter control, it is possible to obtain exposure times as low as 0.05 second with the addition of a secondary shutter. This device consists of a three-position shutter that is driven in synchronism with the primary shutter so as to obtain 100 per cent liquid diversion in position A, zero diversion in position B, and 100 per cent diversion in position C. By driving the secondary shutter through this sequence of positions on three successive revolutions of the primary shutter, the collector is exposed to a single pass of the slot rotating at a preset speed.

Two complete and separate nitrogen-pressurized, liquid-supply systems provided individual control of each stream and sources for different liquids. One system included a temperature bath and

provision for mixing liquids prior to transfer to the pressure system. A sump for collecting sprayed liquids for possible reuse was also an integral part of the system.

Two photographs of each collected sample were obtained to provide a permanent film record and to facilitate the reduction of the data. For this purpose the spray booth was equipped with an integral illumination system that could also be used as a light source or background for photographing sprays. The camera used for all still and flash photographs was a 4x5-inch Speed Graphic.

High-speed flash photographs of streams and sprays were obtained with a 1.0-microsec flash unit using GE FT-27 flash tubes. The high-speed motion pictures were taken with a Fastax camera using photospot illumination.

IV.   ORIFICE INSERTS AND STREAM CHARACTERISTICS

In the initial phases of this investigation it was realized that the results obtained and particularly the usefulness of the data were irrevocably dependent upon prior knowledge of the dynamic characteristics of free streams. It is imperative that the important characteristics of such streams be defined and controlled to the extent that they may be predicted. Appreciation of the magnitude of this problem deepened considerably as the program progressed.

Most of the previous investigations on jets and free streams have been primarily concerned with the characteristics which determine a good fire-fighting stream, i.e., "throw" of the stream and nozzle-discharge coefficients. Freeman (Cf. Ref. 5) conducted an extremely comprehensive investigation of this problem to which some information was added at a later date by Blair (Cf. Ref. 6). A similar study was also conducted by Howe and Posey (Cf. Ref. 7), who extended the measurements by evaluating the dispersion of the stream as a function of distance using a sampling technique. However, with the exception of one set of data reported by Freeman to show the velocity profile which was attained by the jet produced by a particular nozzle at its exit, none of these investigators evaluated free-stream characteristics as such.

The criteria to be used in defining a suitable stream were in part arrived at on a strictly arbitrary basis and were in part evolved on the basis of indirect experimental evidence. The arbitrary requirements may be summarized as follows:

1.   The jet diameter should be equal to the orifice diameter and should retain this same average dimension in the free stream for distances that are large relative to orifice diameter or impingement distance; i.e., the maximum tolerable spread angle is of the order of minutes.

2.   The jet must be stable. In particular, it must be directionally stable so that

direction of flow does not change with time; also it must be continuous in the sense that mass rate is neither intermittent nor variable with time. Adherence to these conditions precludes the presence of separation and/or cavitation within the orifice itself.

A less obvious but even more important requirement for a good free stream involves the specification of the free-stream velocity profile. Although the controlling parameter could be momentum rather than velocity, the information available does not warrant a distinction. In any case, the two factors have dynamic similarity for any given system if it is assumed that the stream is a continuous medium. Since the concept of the free-stream velocity profile was attained through a strictly empirical approach, and since the method of evaluation is at best an indirect one based upon hypothesis, some benefit may be gained through a discussion of the chronological development of the orifice design that apparently produced streams having symmetrical and similar free-stream velocity profiles.

Using the data of Rouse and Hassan (Cf. Ref. 8) to obtain monotonic entries and the unpublished results of an investigation on orifice characteristics,* streams that were apparently stable were obtained with the short, smooth-bore orifices specified for orifices 2A, 9A, and 9B of Table II. In order to provide monotonic entries over a range of diameters from 0.040 to 0.125 inch with a minimum amount of tooling and yet conform to a maximum insert diameter of 0.312 inch (limited by the design requirements of the barrel assembly), elliptical contours were provided for the larger sizes. The contour was the same for sizes from 0.085 to 0.125 inch and was based on a 0.125-inch diameter with $a/r = 4.0$ and $b/r = 1.0$. For orifices having 0.040- through 0.0785-inch diameters, a 0.113-inch radial entry was adequate. In all cases the diameters were held to standard reamer tolerances, and the contours to the usual ground tool surface, i.e., with surface irregularities of approximately ± 0.001 inch. The comparatively short straight orifice lengths used for all orifice sizes from A through D were the results of an attempt to obtain stable streams with high discharge coefficients and minimum physical size. The first indication that these specifications were not adequate became apparent when it was found that the spatial distribution attained by the spray which was formed by a pair of impinging streams produced by such orifices was not symmetrical or reproducible and would not retain similarity for orifice Reynolds numbers of 20,000 and larger.

There is no mathematical basis for the requirement that the spray cross section be symmetrical; on the other hand, if the components of the system have geometrical symmetry and are dynamically balanced, it is difficult to perceive how nonsymmetry could be a logical consequence of the impingement process. In fact, since the radial-velocity components of the spray particles are the result of a random multiple-particle collision within the impingement zone, the dispersion attained should follow a statistical pattern and more specifically a near-normal distribution pattern. Thus the mass distribution of the spray as evaluated by the sample obtained should approach a true Gaussian distribution. Fortunately experimental evidence has served to confirm this line of reasoning.

---

*This work was carried out at this Laboratory by Glen W. Maxwell during 1950 and 1951.

The orifices as first designed were apparently adequate from the standpoint of stream stability, at least in so far as it was possible to distinguish a stable stream from an unstable one by visual and/or photographic methods. Thus the streams were in essence directionally stable and were circular in cross section with a maximum spread angle of about 5° even though considerable flare was exhibited at or near the orifice exit. Preliminary sampling indicated that a random and low-frequency inconsistency produced spatial distributions that could not be duplicated. Figure 7 shows three samples obtained with the same set of orifices using water as the test liquid. Views A and B illustrate the extreme variation of ten samples obtained with identical operating conditions, whereas view C is typical of the marked variations obtained as the jet velocities increased. Though some change in spatial distribution might be expected with increasing jet velocity, the curve should at least retain a characteristic shape. Close examination of the streams in the transition region near the orifice exit showed that the striations formed at the end of the transparent stream varied in time and position around the circumference of the stream and perhaps indicated a less obvious type of instability. On the basis of the work done by Maxwell, it was believed that such instabilities could be attributed to the presence of large-scale turbulence and/or cross velocities at the orifice entrance. Thus the baffle and the turbulence-reducing screen shown in Figure 3 were added to the barrel assembly. With this configuration it was found that excellent duplication could be maintained. (It was also necessary to have the barrel assembly completely air-free at all times.) Figure 8 shows two photographs of different samples taken at the same cross section of a water-water spray and represents the extreme variation obtained in six successive samples. In most cases, if one of the photographs were superimposed on the other, the appropriate menisci would almost coincide. The excellent duplication thus shown was also obtained at the higher jet velocities, but the characteristic curve of spatial distribution changed appreciably with jet velocity.

Attempts to rationalize this apparent anomaly led to the hypothesis that nonuniform velocity profiles can occur in free streams. If it is assumed for the moment that such velocity profiles can exist, it must also be concluded that free-stream velocity profiles may be either nonsymmetrical or nonsimilar or both. It is immediately apparent that impingement of two such streams will probably result in a nonuniform momentum exchange and hence in nonsymmetrical, distorted, and inconsistent spatial distribution of the resultant spray. The impingement of such streams may be analogous to the impingement of idealized streams having different diameters, different moments, and/or varying degrees of misalignment.

If it is also assumed that nonsymmetry of the velocity profile attained in the free stream is primarily a function of the physical configuration of the orifice-barrel assembly and that the profile is stable with time as indicated by the consistency of successive samples, it should be possible to observe a consistent change in mass distribution as one complete orifice-barrel assembly is rotated about its axis. Under these conditions the degree of departure from a symmetrical curve should at least pass through a minimum as the optimum impingement position is approached. This optimum curve will also be affected by the similarity of velocity profiles of the two streams as well as by the relative position of the profile maxima with respect to the geometry of the sampling system.

The effect of the distorted velocity profiles is graphically illustrated in Figure 9. As just indicated, these samples were obtained under nearly identical operating conditions with the exception that one complete barrel assembly was rotated about its axis and the other remained fixed. Since these curves were reproducible, it was concluded that stable, nonsymmetrical velocity profiles do exist and that the distortion obtained is directly associated with the orifice-barrel assembly. It was also possible to conclude that the variation in spatial distribution as determined by these sampling methods is a very sensitive although indirect method of evaluating free-stream velocity profiles.

Early attempts to attain uniform and symmetrical velocity profiles by the more obvious method of eliminating surface roughness and upstream discontinuities were quite disappointing. In fact, after the orifice surface was carefully lapped and polished, and the orifice-barrel junction was contoured, the streams became violently unstable and the cross section markedly noncircular. In an effort to explain such an unreasonable reaction, it is necessary to re-examine the flow conditions actually existing in the orifice inlet and the orifice section and, with considerably less sureness, within the free stream itself.

The classical concept of flow conditions (Cf. Refs. 9 through 12) within the transition section of a smooth entry of a pipe pictures a near-uniform velocity profile immediately after acceleration with an extremely thin laminar boundary at the tube wall. If it is assumed that the energy loss through the transition is negligible, the mean and local velocities at this cross section are identical and equal to the theoretical velocity $\sqrt{2g\Delta P/\delta}$, where $\Delta P/\delta$ is the change in static head. If the contraction section is succeeded by an appreciable tube length, retardation takes place at the walls, and a laminar boundary layer begins to form. Continuity of mass transfer requires that the decrease in velocity near the wall be accompanied by an increase in velocity at the center. This requirement in turn predicates mass transport toward the center of the tube with an accompanying radial-pressure gradient. If the process is allowed to continue for an appreciable distance (some 300 to 400 pipe diameters) at Reynolds numbers below the critical value, the flow configuration becomes stable, and the radial-pressure gradients practically disappear. For the case where the flow is incipiently turbulent, i.e., with Reynolds number considerably in excess of the critical value, the laminar flow in the boundary becomes unstable before this condition is reached, further boundary-layer growth taking place in accordance with the principles of turbulent boundary layers. A stable velocity profile with negligible radial-pressure gradients will be attained after some 50 diameters, the flow being turbulent except for a thin laminar sublayer along the walls.

Rouse (Cf. Ref. 10) discusses the effect of surface roughness upon the final and stable velocity profile, and Shapiro and Smith (Cf. Ref. 13) illustrate the effect of a single surface discontinuity on friction coefficients, but little information is available regarding the promotion of turbulence due to surface roughness or discontinuities. Although it is generally presumed that the transition from laminar flow to turbulent flow follows an axially symmetrical pattern, it is extremely doubtful

that such a condition is attained in a practical case. It is more likely that the local imperfections on the surface produce nonsymmetrical transitions and therefore nonsymmetrical velocity profiles within the transition section. As such irregularities are reduced in number and frequency by lapping and polishing, it actually becomes possible to accentuate the nonsymmetry. This fact may serve to explain in part the apparent anomaly mentioned.

If the configuration of the usual rocket injector orifice is now considered to be limited to L'/D ratios of the order of 3 to 10 and is required to operate at Reynolds numbers well into the turbulent regime, it is seen that the transition from laminar to turbulent flow is barely initiated at the time the jet leaves the confines of the orifice walls. The combined effects of radial-pressure gradients, elimination of wall drag, and nonuniform turbulence initiation suffice to produce streams having unpredictable dynamic characteristics as well as a considerable amount of breakup and dispersion.

In the light of this discussion there are two obvious approaches to a solution of the practical problem. First, it appears possible to produce suitable streams with very short contoured orifices or sharp-edged orifices which essentially eliminate the possibility of transition. Unfortunately the stream stability is highly susceptible to very slight fluctuations in upstream conditions, and therefore such streams are unsuitable for the practical case (Cf. Refs. 14 through 16). Second, if orifice lengths were increased to provide L'/D of 50 or more, it should be possible to produce adequate streams. Again practical limitations impose serious difficulties though not as serious as when the first method is used. The alternative that proved most fruitful resulted from an attempt to obtain a fully generated turbulent velocity profile in the free stream within the available 4 to 6 diameters of orifice straight section by introducing a uniformly rough surface that would accelerate the transition to turbulent flow. For this purpose a No. 0-80 tap was run through a pair of orifices of 0.052-inch diameter to produce a surface-roughness factor of about 6.5 (ratio of radial height of roughness to minimum orifice radius).

The improvement thus obtained in both stability and consistency of spatial distribution was remarkable, but subsequent sampling showed variations amounting to approximately 10 per cent of local mass rate as the relative position of stream impingement varied. Although this improvement represented several orders of magnitude, it was believed that the influence of variations in stream characteristics should be eliminated in so far as possible. Thus a new series of orifices was fabricated in which the straight section of the orifice was increased to about 20 diameters (Cf. Table II) in order to provide additional time for smoothing of the velocity profiles prior to the orifice exit. Two orifices having 0.052-inch diameter were tapped 0.37 inch (24 turns of a No. 0-80 tap) from the entry end and then reamed and retapped to assure a clean edge to the partial thread. Samples were obtained with water over a range of Reynolds numbers and for a number of impingement configurations to yield the distribution curves shown in Figures 10 and 11. In Figure 10 the Reynolds number varies from 18,000 to 53,000; though some distortion is apparent at the higher values, the

same basic characteristics are retained throughout this range. The curves shown in Figure 11, when compared with those of Figure 9, show considerable improvement; though perfection was not attained, it was decided that the characteristics of the streams thus produced and evaluated were suitable for the investigation of the liquid-phase mixing of a pair of impinging streams.

The effect of surface roughening on the visual characteristics of free streams is graphically illustrated in Figure 12. The photographs were taken with a 1-microsec flash. View A shows the streams produced by two 0.052-inch diameter orifices fabricated to the same specifications but without surface roughening. View B shows the jets produced by the same orifices operating at the same pressure drop after the inlet end had been tapped a distance of 0.312 inch to produce a surface having a roughness factor of 6.5.

It is interesting to note that the glassy section of the stream appended to the orifice exit in view A of Figure 12, which might be associated with the laminar boundary layer, completely disappears when surface roughening is introduced. Perhaps even more startling is the fact that the degree of jet breakup attained with the turbulent stream is markedly less than is produced by smooth-walled orifices. Although a velocity differential (therefore a slight change in air drag) exists because of a nominal 10 per cent decrease in the discharge coefficient of the tapped orifice, it hardly accounts for the illustrated differences.

High-speed flash photographs of sprays produced by fully turbulent streams reveal only minor differences when compared with sprays produced with incipiently turbulent streams. Views A and B of Figure 13 show the minor and major axes, respectively, of a spray produced by water streams from two orifices (10G-T and 10E-T) without any specific turbulence-inducing devices operating at a pressure drop of 100 psi. Figure 14 presents photographs obtained under conditions similar to those of Figure 13 except that the orifices had been tapped to promote fully turbulent streams. It is fairly obvious that some change in distribution is obtained, and it might even be stated that the waves visible in view A of Figure 13 have been nearly eliminated. This latter statement is open to argument depending upon an individual interpretation, but it indicates that stream characteristics could have considerable influence on the fineness of a spray such as those observed by Heidmann and Humphrey (Cf. Ref. 17).

Time did not allow a comprehensive investigation of the influence of orifice configuration on stream characteristics, and though few or no quantitative data were obtained, some of the more pertinent experimental findings may be summarized as follows:

1. Turbulence-inducing devices tend to promote directional stability, reduce effects of upstream disturbances, and promote symmetry of the velocity profile.

2. Excessive surface roughness can produce a considerable amount of flare without appreciable effect on the other stream characteristics (based on one test with a roughness factor of 3.5).

3.   Thread forms are only one type of roughness that may be used, and it was indicated from tests on one series of orifices that a single concentric surface discontinuity would be adequate if it could be made sufficiently uniform.

4.   Minimum values of L'/D and of surface roughness required to produce symmetrical velocity profiles have not been determined but probably are less than the values used in these experiments.

5.   In general, the discharge coefficient may be expected to be reduced approximately in proportion to the length of the turbulence-inducing section and to the over-all orifice length.

6.   Many of the common difficulties of stream misalignment due to fabrication are nonexistent for fully turbulent, symmetrical, and stable streams. The significance of this statement in respect to its practical applications cannot be overemphasized.

7.   A stable, controlled velocity profile is prerequisite to predictable mass distribution in the spray resulting from a pair of impinging streams.

V.   EXPERIMENTAL PROCEDURES

Each spray condition was evaluated by compiling the data from a number of different samples so that the flow rate for the entire spray cross section was taken into account. The same end result could be obtained either (1) by rotating the collector about its axis so that the sample in each tube was considered to represent the local flow rate within the section of an annulus or (2) by moving the collector in such a manner that the entrance of one bank of tubes fell on successive great circles having a common diameter which was perpendicular to the plane of the stream center lines and which passed through the impingement point. Although the latter method produces more complete information with a smaller area correction, the relatively large number of samples required and the increased complexity of the collector mounting led to the use of the former technique. The mixing factor of one set of data using the rectangular sampling method is included in Table III, and it is seen that there is no significant difference between that value and one obtained by the polar method as used in all the other sampling. The angle θ was defined as the angle of rotation of the collector about its axis from an arbitrarily defined reference position; $\theta = 0°$ was taken for the collector position wherein the B-D axis was in the plane of the stream center lines. (The A-C axis was aligned along the major axis of spray having an elliptical cross section.) The orifice represented by subscript 1 was always placed on the same side of the spray as the B arm of the collector when $\theta = 0°$. (Similarly subscript 2 represents the orifice positioned on the same side of the spray as the D arm of the collector.)

For purposes of evaluating a given spray condition, six samples were obtained for collector

positions of $\theta = 0, 15, 30, 45, 60$, and $75°$, the rotation being clockwise as viewed from the impingement point. Thus, if a spray were symmetrical in cross section and had a cone angle of $100°$, it would be possible to sample over 600 individual points. In practice such a spray is rare, and for these experiments it was found that the total number of points actually sampled seldom exceeded 350.

Two 4×5-inch photographs of the sample were obtained, each containing a single continuous bank of collector tubes, i.e., two radial arms of the collector. Thus a series of six samples produced the data shown in Figure 5.

Although the quantity of fluid obtained in each tube is directly proportional to the local mass rate, the use of polar sampling requires that each tube represent a different total mass rate which is equal to the mass of the sample actually collected multiplied by an area correction factor C defined as the ratio of the area represented by the sample A_s to the tube area A_t; i.e., $C = A_s/A_t$. In the case of the center tube the same sample is obtained six times, and some overlap is encountered in the first tubes of each radial arm. Thus the correction factors are less than 1.0 for these tubes. The sampling area was taken as that portion of the area of a lune which has a dihedral angle of $15°$ and its axis coincident with the spray axis and which is bounded by the intersection of two cylindrical surfaces having their axes coincident with the spray axis. The radius of the central cylinder is equal to 0.125 inch, and successive cylinders have radii increasing in 0.250-inch increments. The area correction factors obtained in this fashion are itemized in Table II. It may be noted that the correction factor becomes quite large near the periphery of the spray, tending to amplify the errors involved in measuring relatively small column heights. However, the gross effect was usually quite small since compensation was obtained by weighting the data on the basis of the percentage of the total flow rate represented by any one sample.

Stream alignment was attained under flow conditions in two steps. First, each stream was positioned with its vertical center line coinciding with the center line of the collector; thus the stream continued to lie in the plane of the collector tubes (for $\theta = 0°$) as the barrel assembly was moved along its track. Second, a minor adjustment was made of the barrel mounting assembly so that the spray formed by impingement was symmetrical about the plane of the stream center lines. This adjustment was accomplished with sufficient accuracy by visual observation of the spray fan above the impingement point.

The sample was obtained by exposing the collector to the spray with one or more passes of the shutter. A comparison of samples obtained with various numbers of exposures indicated that there was no significant shutter effect. Under certain conditions a small quantity of spillover appeared in the collector but normally was easily recognized as such and thus could be ignored.

Between samples the collector was thoroughly washed, rinsed in a detergent solution, and allowed to drain for at least 5 minutes. With this procedure the tendency for the tubes to trap air during the filling process was eliminated, and yet no measurable residue was retained on the tube walls.

A reference pressure drop of 100 psi was arbitrarily chosen as a reasonable value for establishing a level of operation, and most of the data are relative to this value. For example, as momentum ratio was varied from 0.4 through 1.67, the pressure drop across one orifice was always maintained at 100 psi. Although any one of a number of other criteria could have been established (such as constant total flow rate, a fixed mass rate for one orifice, etc.), fixing the pressure drop was convenient since for any given configuration the momentum ratio is directly proportional to the pressure-drop ratio.

Two photographs were obtained of each sample to produce histograms of the mass distribution attained along two great circles. The individual column heights thus obtained were proportional to the local mass rate, and in the case of immiscible liquids a dual distribution was obtained that could be used to evaluate local mixture ratios. The negatives were projected onto a ruled grid at original size in order to evaluate the column heights. Calibrated metal rods used to determine the accuracy of this technique showed that readings greater than 1.0 inch were in error by less than 1 per cent and that smaller values could be determined within ±0.010 inch.

VI.   SPRAYED FLUIDS

The bulk of the data was obtained with the two immiscible liquids, carbon tetrachloride and water. The CCl_4 was 99.9 per cent pure, and water was city tap water with a small quantity of water-soluble nigrosine (0.015% by weight) added in order to provide contrast for photographing and analyzing the samples.

In one series of samples kerosene was substituted for the CCl_4 as a one-point check on the effect of liquid density. The effect of miscibility was determined using water and dyed water (Cf. Section VIII-C).

The numerical values of physical properties of the liquids used throughout these experiments are presented in Table V. In no case was any correction for temperature or pressure applied since such changes were small and would have a negligible effect on the results obtained.

VII.   EVALUATION OF SAMPLES

In the course of the experiments nearly 600 samples were obtained as a means of evaluating 100 different test conditions. On the average each sample represented data at some 50 different points in the spray; thus the local mass rate and local mixture ratio were evaluated for record approximately 30,000 times. It is obvious that the presentation of such data by direct plotting would render them incomprehensible and that the usefulness and possibility for correlation of the information are dependent upon a simplified

method of evaluation.

A.   Mass Distribution

The mass distribution attained in a spray has significance only in association with a particular geometrical configuration. In most practical cases, predetermined design specifications have considerable bearing on the importance of these spray criteria. For example, it might be required to produce a uniform mass distribution at some particular cross section of a rocket motor having a triangular-section combustion chamber. Such a configuration (or any other for that matter) could conceivably be attained with a single injector but more likely would be approximated with multiple units in one of an infinite number of ways. Thus the possibility of defining an optimum distribution pattern for a single spray for all uses is excluded. In one sense, at least, this is a fortunate situation since it permits the variations in mass distribution to be ignored as injector operating conditions vary. It is necessary to presume only that a combustion chamber could be conceived which would provide a required over-all mass distribution with the spray configuration required for optimum mixing (Cf. Section I). Thus no attempt has been made to assign a quantitative value to mass distribution in itself although certain qualitative correlations of distribution as a function of injector-stream dynamics appear permissible (Cf. Section VIII-A).

B.   Variation of Local Mixture Ratio

If it is assumed that the ideal spray is one in which the local mixture ratio is constant and equal to the input mixture ratio, then any actual spray may be compared with the ideal case by noting the departure of the local mixture ratio from the nominal value at a number of different points within the spray. If the number of points examined is sufficient to account for the entire spray volume, it is possible to determine an average value of this difference that is indicative of the degree of mixing attained in the spray. Thus

$$Y = \frac{\sum_{0}^{n'}(R - r)}{n'}$$

The simple average Y as obtained in this manner is inadequate in several respects. First, since the local mixture ratio may take values ranging from zero to infinity, Y has ∞ as one limit even though it may be due to the influence of a single value of local mixture ratio that represents an insignificant portion of the total spray. Second, each sampling point has an equal influence regardless of the proportion of the total spray represented. Third, the absolute value of R can have considerable influence on the magnitude of the summation. These disadvantages may be eliminated as follows:

       1.   By redefining mixture ratio as a weight fraction of one component to the total.
            (In order to be consistent with common practice, the simulated oxidizer appears

as the summator.)

2.   By weighting the mixture-ratio difference on the basis of the fraction of the total sample represented.

3.   By using the ratio of the mixture-ratio difference to the nominal mixture ratio.

Thus a more suitable evaluation is obtained if

$$Y' = \Sigma_0^{a'} \frac{C_w}{W}\left(\frac{R-r}{R}\right)$$

Y' has limits of zero and 1.0; however, since r may be either larger or smaller than R and thereby may have either positive or negative values, Y' is more or less self-compensating and furthermore is dependent upon the actual value of R when $R \neq 0.50$. Both of these characteristics may be eliminated if two terms are used and if it is assumed that the departure of the local mixture ratio toward either limit has similar effect on over-all performance when the mixture-ratio difference represents an equal percentage of the total increment. Thus, if R has a value of 0.8, a value of $r = 0.6$ is equivalent to $r = 0.85$ even though one increment is four times the other. These revisions to the equation for Y' produce the following result:

$$Y'' = \Sigma_0^{a} C\frac{w}{W}\left(\frac{R-r}{R}\right) + \Sigma_0^{\bar{a}} C\frac{w}{W}\left(\frac{R-\bar{r}}{R-1}\right)$$

Y'' is a value representing the departure of the spray from a nominal value; if it is subtracted from 1.0, however, the criterion becomes a measure of the percentage of the spray that can be considered to attain the nominal mixture ratio. In a slightly different conception this value can represent the proximity of the entire spray to the optimum configuration. Converting also to a scale from zero to 100,

$$E_m = 100\left\{1 - \left[\frac{\Sigma_0^{a} C_w (R-r)}{WR} + \frac{\Sigma_0^{\bar{a}} C_w (R-\bar{r})}{W(R-1)}\right]\right\}$$

This, then, is the empirical equation that was used to define a mixing factor E_m based on the variation in local mixture ratio. This factor may be used to evaluate and compare sprays of differing configurations produced under different conditions.

It should be noted that the root-mean-square method was avoided since it tends to accentuate the larger differences which in this experiment were the most inaccurate.

VIII.   PRESENTATION OF RESULTS

The mass distribution and mixing factor of various sprays have been evaluated in order to assess

the relative importance of stream dynamics and configuration. In general, whenever possible, each important variable was investigated independently. When such investigation was not possible, an attempt was made to establish significant trends for a given configuration and to verify such trends for other configurations with a minimum amount of data as changes were made.

The more important parameters investigated include momentum ratio, impingement angle, area scale, and area ratio. A cursory investigation of the influence of fluid physical properties, impingement distance, and energy available for mixing was also completed. With the exception of the data on miscibility and one point obtained with kerosene, all of the data were obtained with carbon tetrachloride and water as the sprayed fluids.

A.   Mass Distribution

It is impractical to reproduce here the large number of histograms that represent the variation in mass distribution obtained with various configurations. However, certain general characteristics were evolved that provide considerable assistance in defining the distribution at least in a qualitative manner. It must be remembered that the following statements can apply only to sprays produced by streams having symmetrical and similar free-stream velocity profiles.

Figure 5 shows the elliptical cross section that is invariably obtained for a pair of streams having equal moments and equal effective impingement areas. The change in distribution occurring for any one radial arm may be followed by starting with the right half of the upper photographs for $\theta = 0°$ and continuing similarly through $\theta = 75°$. From this curve return to the right half of the lower photograph for $\theta = 0°$ and again through the series to $\theta = 75°$. Similarly the C arm and the D arm of the collector may be followed through the six positions.

The total-distribution curve obtained along any great circle of the sampling surface when projected to a plane surface approaches a Gaussian distribution, which is symmetrical about the spray axis. A distinction between total distribution and that attained by a single component is necessary since it can be seen that along the minor axis and in varying degrees for other positions (exclusive of $\theta = 0°$) this statement does not apply to a single component. In all cases, regardless of configuration, operating conditions, or fluid properties, this distribution of each component in the plane of the stream center lines was obtained and invariably represented penetration of one stream through the other. Although the quantity of fluid involved was small and therefore led to possible inaccuracies in the evaluation of local mixture ratio, it was found that a continuous variation of r from 1.0 to 0 existed across the B-D axis with the maximal value occurring along the resultant momentum line. Thus at no time was it possible to attain the optimum. The hypothesis states that optimum mixing will occur at an impingement angle of $180°$; however, the limitations of the equipment did not allow an investigation of this configuration. No really satisfactory explanation of the penetration phenomenon has been suggested; therefore it must be ignored for the present. Since the process was consistent and reproducible, it can be assumed to be characteristic

of stream impingement and therefore in itself has no appreciable influence upon the results obtained in this investigation. In contrast to the penetration phenomenon it should also be noted that, for sprays produced by streams of equal momentum and area ratio, the local mixture ratio along the major axis was nearly constant and equal to the nominal value. In actual experiments this condition was not attained exactly, but the trend was consistent, and the variation in mixture ratio was small enough to allow the assumption that such would be the case for truly ideal streams.

The most significant change in mass distribution was obtained as momentum ratio was varied. Although Figure 15 includes the photographs for $\theta = 0°$ only, it can be seen that the maximum local mass rate shifts along the $B-D$ axis in the direction of the high-momentum stream. As this shift takes place, the spray cross section assumes a kidney shape that is symmetrical about the $B-D$ axis only. A similar distribution change occurs as the area ratio departs from 1.0 because of the misimpingement of portions of the larger stream. The limits of the effect of nonsimilar effective area ratios can be visualized when a stream the size of a pencil lead impinges upon a second stream 1 inch in diameter with the same total momentum. The small high-energy stream serves as a splitter for the large stream emerging nearly undisturbed from the impingement process. Increasing the momentum of the large stream is perhaps helpful up to the point where that portion of the large stream that is effective in the collision process has momentum equal to the small stream. However, the total momentum of the large stream is very large at this point; thus the possibility of equal momentum exchange is excluded.

The change in spatial distribution produced by varying the impingement angle α is illustrated in Figure 16. Again only the samples for $\theta = 0°$ are included. As might be expected, the included angle of the spray along both major and minor axes increases as impingement angle increases. More important, however, is the fact that the distribution retains the characteristic Gaussian shape. It may be noted that the collector was inadequate for the higher impingement angles, necessitating some extrapolation of the curves to the spray limits at or near the major axis. For this reason the bulk of the data on other variables was obtained with an impingement angle of 60°. In interpreting data of this type it is necessary to remember that these histograms show local mass rates on a spherical sampling surface. There is a tendency to disregard (1) the effect of projecting the distribution curve to a plane as accomplished by the collector and (2) the relatively large total mass represented by the outer tubes.

By generalizing considerably on the data obtained, it is possible to make at least two statements that may assist in utilizing the information in a practical application (obviously such generalities must always be considered as inferior to and in lieu of more quantitative, discrete information):

1.   For a pair of impinging streams wherein the total momentum ratio is 1 and the configuration is such that equal portions of the momentum available for mixing is dissipated in the impingement process, the mass distribution along any great circle of the sphere having its center at the impingement point and passing through the resultant momentum line may be defined by a Gaussian equation.

2.   Penetration of the fluid of one stream by the other is a characteristic phenomenon and is amplified by inefficient impingement configurations because of unequal momenta and/or unequal effective impingement areas. Under these conditions the spray cross sections obtained are distorted and nonsymmetrical.

B.   Variation in Mixture Ratio

The variation of local mixture ratio was evaluated by the determination of E_m over significant ranges of six distinct variables: (1) momentum ratio M_1/M_2; (2) impingement angle α; (3) area scale A_1/A_1'; (4) area ratio A_1/A_2; (5) impingement length L; and (6) fluid physical properties. The parameters that serve to identify the geometrical configuration of the spray and conditions of operation are included in Figure 1 and Table III. A typical set of data, determined for one sample and including the necessary calculated data, is shown in Table VI. A detailed summary of the results obtained is also presented in Table III.

The consistency of the data and probable variation due to experimental difficulties are indicated in Table VII, where data for six different series of samples are summarized. The first three values were obtained with the same set of orifices at different times but under as nearly identical operating conditions as possible. The last three values were obtained with similar operating conditions but with a different set of orifices and various relative configurations of one orifice to the other. In general, the agreement is considered quite good even though in one case the deviation represents nearly 2.5 per cent of the average. As can be noted in Table III, similar checks have been made for other configurations.

1. E_m vs M_1/M_2. Using a particular pair of orifices, i.e., 10E-T and 10F-T (Cf. Table II), an impingement angle of 60°, an impingement length of 0.5 inch, and a reference pressure drop of 100 psi, E_m was determined for values of M_1/M_2 varying from 0.4 to 1.67. These data are plotted as the solid curve in Figure 17, and it is seen that the maximum value of E_m (hence optimum value) occurs very near $M_1/M_2 =$ 1.0. By definition E_m must approach zero as a lower limit as the momentum ratio approaches either zero or infinity, this fact producing the skewed curve above. By plotting the reciprocal of the momentum ratio (symbol x in Fig. 17) it is seen to be immaterial which way the ratio is written, as the same basic curve is retained. A normalized version of this curve plotted as a function of $1/[1 + (M_1/M_2)]$ shows (the dashed line in Fig. 17) the symmetry of the effect about the optimum value 0.5 (when $M_1/M_2 =$ 1.0) and also points to the practical implication that liquid-phase mixing is relatively insensitive to momentum ratio at or near a momentum ratio of 1.0. Contrarily any injection system becomes progressively dependent at an increasing rate on other mixing mechanisms as the momentum ratio approaches either limit.

2. E_m vs α. The influence of impingement angle on E_m was also determined with orifices 10E-T and 10F-T. The range of impingement angles available with the impinging-jet assembly was not as large as might be desired but included most of the values encountered in the usual rocket design. Figure 18

shows the variation of E_m with α for two different momentum ratios; i.e., $M_1/M_2 = 1.0$ and 0.6. Within the range and scatter of the data a suitable correlation can be obtained with straight lines, indicating that better mixing is obtained at lower impingement angles and that regardless of impingement angle better mixing is obtained for a momentum ratio of 1.0. A combustion correlation showing increasing performance for α decreasing from 90 to 45° was obtained by Aerojet (Cf. Ref. 18) for a range of α from 45 to 120°. In addition, Aerojet showed, by extending the range through 120°, that minimum performance was obtained for $\alpha = 90°$. (In this report α is equivalent to γ as used by Aerojet.) Unfortunately the data obtained from the tests reported herein cannot substantiate this fact or refute it. In this case it must be assumed that mixing is dependent not only on the momentum (or kinetic energy) available for mixing but also on the time required for penetration. Obviously from a strict geometrical viewpoint penetration time approaches a minimum for $\alpha = 90°$, increasing as α changes in either direction. Considering also the fact that the mixing factor must approach zero as the impingement angle approaches zero, there must be a maximum value between 45 and 0° that would also be an optimum value and may or may not be secondary to the hypothesized optimum occurring at $\alpha = 180°$. Since the slope of the curve obtained is rather low, the benefit to be expected is rather small and therefore did not appear to justify the additional experiment necessary to define this optimum.

It should be noted that the values of E_m obtained for α of 70 and 80° are probably in error to some extent because of the fact that a portion of the spray was not sampled [Cf. Fig. 16 and the $(\Sigma\,Cw)/w$ column of Table III]. The missing portion consists of the outer ends of the elliptical section wherever the spray-cone angle exceeded 100°, the maximum intercept angle of the collector. Since this portion of the spray is along the major axis and is normally at or near the nominal value, E_m as calculated would be somewhat low. In order to eliminate the possibility of this effect appearing in other data and yet to obtain the maximum permissible spray cross section, an impingement angle of 60° was used for evaluating other parameters.

3. E_m vs impingement distance. If it is assumed that the streams retain a cylindrical cross section from the orifice exit to the impingement point and that dynamic conditions are not changed over this distance, there appears to be no logical reason why the impingement distance (distance from orifice exit to impingement point) should, in itself, have any influence on liquid-phase mixing. Three different impingement lengths of 0.25, 0.50, and 0.75 inch produced E_m values of 74.87, 75.45 (average of six series), and 73.91, respectively, to substantiate this statement for the condition where $M_1/M_2 = A_1/A_2 = 1.0$. In all other configurations the impingement distance was fixed at 0.5 inch.

4. E_m vs area scale. A determination of the effect of the scale of orifice area on liquid-phase mixing was prerequisite to the investigation of the effect of diameter ratio.

Four pairs of orifices (three in addition to the pair used to obtain the data on momentum ratio, impingement angle, and impingement length) were used for this portion of the investigation to cover a range of areas from 1.258×10^{-3} sq in. through 4.86×10^{-3} sq in. Based on the area of the smallest orifice of the series, these orifices provide area-scale factors of 1.0, 1.75, 2.50, and 3.75. In all cases

the orifices were provided with monotonic entries, a turbulence-inducing roughened surface for approximately 5 diameters from the entry end, and a total length of about 22 orifice diameters. The fabrication details are summarized in Table II.

Before attempting to evaluate the liquid-phase mixing, the spatial distribution of the spray formed with each pair of orifices was utilized to indicate the symmetry and similarity of the dynamic characteristics of the two streams at the point of impact. For this purpose, water was used in both streams, and it was assumed that the mass distribution of the liquid in the spray must attain a near Gaussian distribution along both axes of the elliptical cross section. Furthermore, since it was intended that the streams should by symmetrical, it was required that this same distribution be retained for any relative position of the two streams. Thus the spatial distribution of the spray was determined for an initial reference position, and subsequent samples were obtained for different radial positions of each complete barrel assembly; when necessary, the surface roughness of the orifices was adjusted until all samples of such a series were nearly identical. After the symmetry and similarity of the free-stream dynamics were thus established, samples were obtained with carbon tetrachloride and water in order to evaluate the liquid-phase mixing.

The mixing factor was determined for each pair of orifices for three momentum ratios at an impingement angle of 60° and for three impingement angles at a momentum ratio of 1.0. The data are plotted as a function of an area-scale factor in Figure 19. Although the limits are not defined and the changes in mixing factor are small compared with area changes, the nearly linear trend toward higher mixing factors with orifice area is apparent and cannot be ignored for the case where the momentum ratio is near 1.0. In the case of the data for momentum ratios of 0.6 and 1.67, the scatter of the data is larger than the change due to a possible trend, and a best fit may be obtained by drawing a single straight line of zero slope for both sets of data.

The fact that a scale effect was obtained not only complicates the analysis of area-ratio data but is also quite difficult to explain. One might suggest that the available energy is utilized in a more efficient manner as the stream diameter increases or that the increase in kinetic energy available for mixing and/or the increase in Reynolds number influences both scale and magnitude of stream turbulence so as to increase mixing. However, neither possibility can be verified until more suitable experimental techniques are available. There is also the possibility that the experimental data are in error, but in view of the similarity in slope for the curves obtained at three different impingement angles and the consistency of these data with that obtained on impingement angle and momentum ratio, the possibility seems rather remote. At this writing it can only be concluded that, for otherwise optimum conditions, a scale effect exists and over the range investigated is evaluated by the data presented in Figure 19.

5. E_m vs area ratio. As has already been pointed out (Cf. Section II), the cross-sectional area of the streams has significance only to the extent that it might determine that portion of the stream which is effective in the impingement process. In the case of a single pair of streams of circular cross section, this effective area must be directly proportional to the stream cross section; thus within these

restrictions a correlation with a relatively simple criterion is permissible.

Combining individual orifices of different sizes from the same four pairs of orifices which were used to evaluate the effect of area scale resulted in area ratios varying from 0.261 through 1.690 in eight steps. Data were obtained on each pair for the conditions where $M_1/M_2 = 1.0$ and $\alpha = 60°$. Although this procedure required the combination of orifices of appreciably different scale, the order of magnitude of the previously determined scale effect could hardly account for the scatter and inconsistency of the data shown in Figure 20, where E_m is plotted as a function of area ratio. Since it had already been demonstrated (Cf. Table VII) that the experimental technique was considerably better than these data might indicate, it was necessary to conclude that some unaccounted-for variable was exerting a relatively large effect upon the results. Extension of the data to cover a range of momentum ratios for two specific area ratios, i.e., $A_1/A_2 = 0.671$ and 0.439, produced the family of curves shown in Figure 21. In the case of the curve for $A_1/A_2 = 0.439$, where only three experimental points in addition to the origin are available, some doubt must remain as to the exact position of the curve. However, in order to be consistent with the other data this curve must take the approximate shape as shown, and in any case considerable flexibility is allowable without materially affecting the remainder of this discussion. Aside from this discrepancy the curves are well established with very little scatter of the experimental points. This factor is important because it shows that consistent data can be obtained as long as a single pair of orifices is used, thereby substantiating the accuracy of the technique. At the same time the data point out at least two possible anomalies in so far as the first hypothesis is concerned. It may be noted that the maximum value of E_m (and hence point of best mixing) occurs for momentum ratios less than 1.0 as the area ratio becomes smaller than 1.0. It is also seen that this shift in the maximum point for a given area ratio is accompanied by an increase in the value of E_m. Considering the maxima for all area ratios, an over-all maximum point apparently occurs in the region where $A_1/A_2 \simeq 0.7$ and $M_1/M_2 \simeq 0.81$.

Although perfectly suitable explanations of these characteristics have not been devised, it is possible to indicate certain mechanisms that could conceivably produce the observed effects. It is fairly simple to rationalize the change in momentum ratio required to produce the maximum value of E_m for area ratios not equal to 1.0 if it is assumed that momentum ratio is actually the controlling factor. Since the area ratios are not the same, a portion of the larger stream is eliminated from the impingement process; therefore the best mixing should occur when the effective portion of the larger stream (i.e., the portion entering into the impingement process) has momentum equal to the total momentum of the smaller stream. Thus, as area ratio decreases, the total momentum ratio for best mixing also decreases. It is quite likely that the effective impingement area varies with momentum ratio; therefore the effect is not linear.

Another apparent anomaly is considerably more difficult to explain; though the mechanism is not entirely clear, it appears to be due to the influence of the kinetic energy available for mixing. Therefore the original assumption wherein the velocity term was taken to be relatively unimportant is not valid. The velocity in itself may have significance since it defines the mean velocity differential that may

exist between the two liquids; indirectly its association with Reynolds number may be indicative of the scale and level of turbulence attained in the stream, which in turn may influence mixing. It seems more likely, however, that a more direct correlation may be obtained if velocity is combined with momentum to give kinetic energy. It should be pointed out that experimental evidence does not indicate that kinetic energy can be used to supplant a momentum correlation since momentum is all important in controlling the impingement process and therefore the mass distribution. It appears more likely that kinetic energy may be used to correlate an effect on mixing that is due primarily to a change in the level or quantity of energy available.

Unfortunately, at least in the light of hindsight, the course of the experiment did not allow for possible changes in kinetic energy. However, calculating the energy available for mixing (defined as the component of the total kinetic energy of a stream that is perpendicular to the resultant momentum line and in the plane of the stream center lines), as was attained by each experimental configuration, yields the family of curves shown in Figure 22. The kinetic-energy term represents the numerical sum of the two components perpendicular to the resultant momentum line referred to the total kinetic energy of a water stream produced by a 0.052-inch-diameter orifice at 100-psi pressure drop. Thus

$$\Sigma(KE)_x = \frac{M_1 V_1^2 \sin\left(\frac{\alpha}{2} - \gamma\right) + M_2 V_2^2 \sin\left(\frac{\alpha}{2} + \gamma\right)}{MV^2 \text{ of reference stream}}$$

Since the kinetic energy as just defined is based on mass rate, it is a specific quantity, having the units ft-lb/sec.

The three curves of Figure 21 have been reproduced in Figure 22, and the kinetic energy available for mixing has been superimposed in order to illustrate the similarity in trends. Obviously the correlation is noticeable and is implied rather than proved; it is clear, however, that the increase in kinetic energy available for mixing could have produced the observed effect. It is also seen that the effects of area ratio and momentum ratio become relatively large as their departure from 1.0 increases.

It is interesting to note that, if the change in area ratio had been obtained by decreasing the area of the water orifice (subscript 1) instead of increasing the area of the carbon tetrachloride orifice (subscript 2), these effects could very well have gone unnoticed. If the implications of the results are extended to this second situation, it is seen that a continuously decreasing value for E_m could be expected and thus would undoubtedly have been attributed to the change in area ratio alone.

Since it appears possible to isolate the effect of kinetic energy merely by varying jet velocity in an otherwise identical configuration (neglecting the possible influence of stream turbulence), a small quantity of data was obtained with this end in view by varying operating pressure drop and liquid properties. Figure 23 summarizes these data in a plot of E_m vs $\Sigma(KE)_x$, which covers a range of pressure drop from 25 through 200 psi with the system CCl_4 and H_2O and included mixing factors for the system

water-kerosene at a pressure drop of 100 psi. Although the system water-water is not strictly similar since it includes the effect of miscibility, one point obtained with this system at 100 psi is also included. In all of these tests momentum ratio and area ratio were fixed at 1.0. It is seen that, even though experimental errors appear to be inconsistently large, the trend of increased mixing with increased available energy is unmistakable. This trend serves to verify the supposed influences of kinetic energy on the data for area ratio (Cf. Fig. 21) and perhaps also indicates one explanation for increased mixing with increasing area scale (Cf. Fig. 19).

The discrepancies between hypothesis and experiment introduced by the data for area scale and area ratio are certainly real and therefore cannot be ignored. However, it was believed that refinement of this investigation to the point where a more rigorous correlation between mixing and stream dynamics is obtained could not be warranted at this time. It would appear necessary to establish the influence of liquid-phase mixing and mass distribution on combustion phenomena before attempting to improve these data. It should also be pointed out that it has been proved a number of times within this investigation (Cf. Figs. 18 through 20) that the detrimental influence of momentum ratios and impingement area become overpowering as either or both of these quantities attain values beyond the approximate limits of 0.6 and 1.67; therefore the exact correlation of the secondary parameters has limited application without effecting the general conclusions.

C. Physical Properties of Liquids

The physical properties of liquids that could conceivably influence liquid-phase mixing include density, viscosity, surface tension, and, when two liquids must be considered simultaneously, miscibility. Density is important because of its influence on stream dynamics and therefore is incorporated in a correlation with momentum or kinetic energy. For most practical applications where dynamic forces of a stream are very large in comparison with surface phenomena, the surface-tension effects can be ignored. Viscosity probably has its most pronounced effect in the portion of the mixing process that is accomplished by turbulent diffusion and/or mass transfer. Since the bulk of the data indicated that these effects were small for the range of the variables encountered, no attempt was made to obtain complete correlations. However, one determination of E_m for $M_1/M_2 = A_1/A_2 = 1.0$ when $a = 60°$ was completed using the system water-kerosene where density ratio was 0.8 and the absolute viscosity ratio was 1.9 (kerosene to water), compared with 1.6 and 1.0, respectively, for the system carbon tetrachloride and water. As was seen in Figure 24, the slight change noted in E_m could be entirely accounted for by the change in kinetic energy.

In view of the lack of knowledge concerning the mechanism that determines miscibility, in particular with respect to rate and proportion (Cf. Ref. 1), and the difficulty in separating mixing of miscible liquids from emulsification of immiscible liquids (a matter of scale only), no attempt was made to obtain a discrete evaluation of the influence of miscibility as such on the mixing process. On the other hand, curiosity and the possibility of major effects led to a three-point determination of E_m using

the system water—dyed water. The mixing factor was determined for three values of momentum ratio, i.e., 0.6, 1.0 and 1.67, with an area ratio of 1.0 and impingement angle of 60°.

In general, the technique used to obtain data on miscible liquids is similar to the method already described (Cf. Section V) for investigating immiscible liquids. However, it is obvious that the evaluation of local mixture ratio must be accomplished in a different manner. The analysis of any one of a number of physical properties of a mixed sample of two suitable liquids would yield similar results (for instance, density, viscosity, surface tension, acidity, etc.), but for present purposes a photometric technique was chosen wherein one component contained a known concentration of water-soluble nigrosine dye and the other remained clear. Thus by determining the dye concentration of a mixed sample it was possible to determine the local mixture ratio. This method had considerable preference since the photometric analysis could be completed while the sample remained in the collector, thereby eliminating the handling problem.

The apparatus shown in Figure 24 is essentially a simple densitometer. The maximum allowable dye concentration, which was determined by the photocell sensitivity and maximum lamp intensity, was somewhat less than 0.1 per cent by weight. Since it was not expected that the maximum concentration would appear in any actual sample, a concentration of 0.1 per cent was used for one component of the sprays. In order to obtain sufficient accuracy (errors of the order of ±1%) it was necessary to be able to evaluate dye concentrations to less than ±0.001 per cent. This sensitivity was obtained by adjusting the photocell to provide a 2-millivolt recorder input for each 0.001 per cent change in dye concentration. The effective range of the photocell was then extended at this same sensitivity by varying the lamp supply voltage in stepwise increments. Judicious use of a neutral-density light filter (6.4% transmission) served to double the range again. A family of calibration curves was then obtained that provided a means of determining the dye concentration of any unknown mixture of water and dyed water (between the limits of zero and 0.1%). With this information the local mixture ratio r could be determined since

$$r = 1 - \frac{B_s}{K}$$

In all cases it was necessary to add a diluent to a portion of the sample in order to obtain a sufficient quantity of liquid for analysis. In addition to the concentration determination of the diluted sample, it was necessary to know the quantity of sample and the quantity of diluent. These data were determined from photographs taken before and after diluting. The photograph before diluting was also employed to determine the local flow rates used to weight the values of local mixture ratio. With these data the local mixture ratio was obtained from the expression

$$B_s = B_m \left(\frac{W_d}{W_s} + 1 \right)$$

This equation is actually a simplified form of

$$B_s = \frac{\overline{W}_d}{\overline{W}_s} (B_m - B_d) + B_m$$

The data obtained with this system are summarized in Table VIII, and it may be seen that, even after allowing for a slight increase in available kinetic energy, the value of E_m for $M_1/M_2 = 1.0$ is higher by nearly 10 per cent than a comparable value obtained with immiscible liquids. Although this increase could be attributed to the effect of miscibility, it is dangerous to make conclusive statements on the strength of these three points. It can be said, however, that the effect shown is certainly in the proper direction, and it is interesting to note that once again the influence of a secondary parameter does not alter the characteristic effect of changing momentum ratio.

IX.   LIQUID-PHASE MIXING AND INJECTOR DESIGN

A rigorous application of the results of this investigation to the design of rocket-motor injectors is dependent upon prior knowledge of the requirements of an optimum combustion configuration. Of particular significance are the specification and determination of certain prereaction conditions that include mass distribution and variation in local mixture ratio. Unfortunately such information is not yet available. However, if the basic assumption is made that optimum injection is irrevocably associated with mass distribution and local mixture ratio, then methods for predicting and controlling these two basic parameters provide in part a sound and logical basis for injector design. This, of course, was the primary objective of this investigation.

In order to apply the results obtained, it is necessary to impose several conditions and to make several other assumptions which can be verified only by combustion experience:

1.   The data are restricted in the sense that they can apply to impinging-stream injectors only. This condition does not necessarily exclude splash-plate and/or deflector-plate injectors.

2.   Although the mass-distribution data may apply to most propellant injectors using impinging streams, the most fruitful application is in the field of biliquid injection.

3.   It is imperative that the streams used in the impingement process have known and controllable dynamic characteristics, i.e., similar and symmetrical velocity profiles in a stable free stream.

4.   It must be assumed that the essential characteristics of a spray produced with

nonreactive liquids in a relatively quiescent system are also produced in a combustion chamber with reacting liquids. This assumption becomes reasonable since mixing lengths of a few stream diameters usually represent mixing times of 1 millisec or less.

5. Optimum combustion occurs for uniform local mixture ratio.

6. The mass distribution can be controlled either by suitable arrangement of multiple sprays or by combustion-chamber configuration.

7. The momentum ratio (total for each propellant) must be equal to 1.0, and the effective impingement areas must be equal to 1.0. (For cylindrical streams, cross-sectional areas are assumed to be significant.)

8. Secondary effects due to impingement angle, area scale, and energy levels can be ignored in lieu of obtaining suitable mass distribution and operating conditions at least until gross effects have been evaluated from the combustion viewpoint.

It can thus be seen that the physical configuration of any injector must be determined by two prerequisites, i.e., $M_1/M_2 = 1.0$ and $A_1/A_2 = 1.0$, and by the chemical properties of a specific propellant combination. The import of the implications of this last statement becomes apparent only when it is realized that with most propellant systems it is impossible to satisfy all of the necessary conditions using a single pair of cylindrical impinging streams.

For example, if an optimum injector is needed for the acid-aniline propellant system to operate at a mixture ratio $r' = 4.0$, the following equations must be satisfied:

$$\frac{M_1}{M_2} = \frac{W_1}{W_2}\frac{V_1}{V_2} = 1.0 \tag{1}$$

$$\frac{1}{r'} = \frac{W_1}{W_2} = \frac{1}{4} \tag{2}$$

$$\frac{A_1}{A_2} = \frac{W_1 \delta_2 V_2}{W_2 \delta_1 V_1} = 1.0 \tag{3}$$

From Equations (1) and (2) it is seen that V_1/V_2 must equal 4.0; in order to satisfy Equation (3), however, if δ_2/δ_1 is taken as 1.5, then V_1/V_2 must equal 1.5/4, or 0.375, obviously an impossible situation. The degree of incompatibility is indicated by the very large discrepancy between the two velocity ratios, i.e., a factor of nearly ten times, and is used here to illustrate one important fact: The usual impinging stream injector is designed as a matter of convenience to conform to a 1:1 impinging stream operating at some

usually not too well-defined injector pressure drop and whatever orifice area is required to produce a predetermined mixture ratio. As far as mixing and distribution are concerned, such injectors cannot be expected to have any similarity to optimum design.

Fortunately the situation is not as hopeless as is indicated since there appear to be at least two approaches to a suitable solution of the problem. These approaches are in addition to the one that assumes a large number of available fuel-oxidizer combinations having very large ranges of specific gravities and hence mixture ratios which would provide means of using a 1:1 impinging stream as an optimum configuration. In the practical case this condition seldom exists (LO$_2$-ammonia being a notable exception), and it is necessary to revert to a more earthy solution. The problem as just outlined is admittedly one of the more difficult though by no means uncommon because of the fact that density ratio is relatively small and that the required mixture ratio is quite large.

The first type of solution consists of a compromise wherein momentum ratio and area ratio are adjusted as necessary to satisfy the equations and yet stay as near as possible to the optimum values of 1.0. It is also possible that mixture ratio could be adjusted without appreciable sacrifice. If Equations (1) and (3) are combined it is found that

$$\frac{M_1}{M_2}\frac{A_1}{A_2} = \left(\frac{1}{r'}\right)^2 \frac{\delta_2}{\delta_1} \tag{4}$$

Substituting values of this problem leads to the conclusion that the product of M_1/M_2 and A_1/A_2 must be 0.094 and that, if they are equal, they would have values of the order of 0.3. Reference to the data of Figures 20 and 21 shows that this combination results in an extremely poor configuration. Reducing the design mixture ratio to 3.0 would help considerably since $(M_1/M_2)(A_1/A_2)$ could be of the order of 0.4, but even this condition is far from the optimum.

The alternative solution is considerably more versatile and probably more effective but has the disadvantage that it requires some extrapolation of the available data. In essence this method takes advantage of the fact that the area ratio involved in the study is the effective impingement area; it is recalled that the cross-sectional area of the stream has significance only for a pair of streams of cylindrical section. Thus in practice it may be possible to use multiple streams of one component impinging on a single stream of the second component or to use streams of nonsymmetrical and nonsimilar cross section. Using the first scheme and returning again to the injector problem with the equation

$$\frac{M_1}{M_2}\frac{A_1}{NA_2'} = \left(\frac{1}{r}\right)^2 \frac{\delta_2}{\delta_1} \tag{5}$$

where A' is the area of one of N holes, it is found that N must be 9+ for $M_1/M_2 = 1.0$ and $r' = 4.0$, or

if $M_1/M_2 = 0.7$ and $r' = 3.0$, then $N \simeq 4$. In order to allow the indicated extrapolation, it must be assumed that the effective momentum interchange between each stream of the multiple array and some segment of the single stream is equal. Obviously the use of circular streams in symmetrical arrangement can only approximate this condition, and it is extremely doubtful that the extrapolation could be carried far enough to justify the use of a 9:1 configuration. However, as can be seen from the accompanying sketch, the use of 4:1 does not appear unreasonable. If each quarter segment of
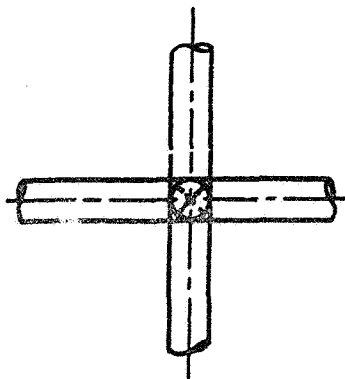
the central fuel stream is considered to act separately, it is seen that the condition of equal area ratio and of equal momentum for each of four pairs of streams has been approximated. It should be remembered that for this propellant system this is at best a fair approximation to conditions for optimum mixing but even so is a far cry from the usual rocket-motor injector. It should also be pointed out that a last calculation (from Eq. 3) shows that the pressure-drop ratio required to attain these conditions is the reciprocal of the area ratio, or in this case 4.0.

The possible configurations of injector designs using noncylindrical streams are nearly unlimited and therefore are not discussed here except to point out that there is no reason to believe that the conclusions presented are not directly applicable to such streams and that this approach to the design of injectors for propellant systems operating at high mixture ratio appears to be the most promising.

It is not intended to imply that liquid-phase mixing and mass distribution are the only factors controlling rocket-motor performance or that adequate control and specification of these characteristics will be a cure-all for most rocket problems. However, the consistency with which most combustion phenomena are associated with the injector and its components is certainly indicative of the importance of injection phenomena as such. Thus it may be concluded that control and correlation of injection processes are prerequisite to understanding the subsequent combustion phenomena. It is hoped that the information presented herein will provide a small part of the necessary information.

X.   SUMMARY OF RESULTS AND CONCLUSIONS

A technique for evaluating the liquid-phase mixing of a pair of impinging streams has been devised, and a number of controlling parameters have been investigated.

In general, it has been shown that the mixing and distribution attained in the spray from a pair of impinging streams having good dynamic characteristics may be optimized in any configuration by controlling dynamic characteristics but that ideal mixing can be attained with only one particular arrangement. The optimum configuration is approached under the following conditions:

1.   The total momentum ratio approaches unity.

2.   The effective impingement area ratio approaches unity.

3.   The impingement angle is approximately 45°. (The experiments indicated only that mixing improved as impingement angle decreased from 90 to 45°.)

4.   The kinetic energy available for mixing approaches a maximum when referred to any predetermined fixed level.

5.   The influence of absolute size of the effective impingement area is small but shows an increasing trend as scale increases.

6.   The effect of impingement length as such is negligible.

7.   Aside from an effect on the hydraulic characteristics of the orifices due to changes in Reynolds number, changes in fluid properties influence mixing only to the extent of the change in stream dynamics.

8.   The variation of local mass rate across any great circle of the spherical surface about the impingement point for a pair of streams of optimum configuration may be defined by a near Gaussian distribution. The cross section of a dynamically balanced spray has an elliptical boundary in the plane perpendicular to the resultant momentum line. Within limits the length of the major axis of the ellipse which is aligned perpendicular to the plane of the stream center lines is a function of impingement angle.

9.   The dynamic characteristics of the free streams have marked influence on stream stability, on spatial distribution, and, to some extent, on liquid-phase mixing. Stream dynamics are controlled by upstream conditions, orifice Reynolds number, and orifice design; the data available indicated that optimum stream pairs require symmetrical, similar (only in lieu of uniform), and stable free-stream velocity profiles.

10. From the limited data available it might be concluded that miscibility is an aid to mixing but does not alter the characteristic effect of varying momentum ratio.

11. The data obtained provide in part a logical basis for rocket-motor injector design.

TABLE I

NOMENCLATURE

a = major semi-axis of orifice entry contour.

A = orifice area (sq in.); subscript 1 refers to a water system, and subscript 2 to a system using an immiscible liquid.

A_s = portion of a spherical surface represented by a sample.

A_t = cross-sectional area of a sampling tube = 0.0227 sq in.

b = minor semi-axis of orifice entry contour.

B_d = concentration of dye in diluent (wt %).

B_m = dye concentration of a diluted mixture (wt %).

B_s = dye concentration of a mixed sample (wt %).

C = area correction factor = A_s/A_t.

D = orifice diameter.

E_m = mixing factor.

g = gravitational constant = 32.2 ft/sec^2.

h = column height (in.).

K = dye concentration in one component (wt %).

KE = kinetic energy per sec (lb) = $MV^2/2$ = $WV^2/2g$.

L = impingement distance.

L' = orifice length.

L'' = length of roughened orifice section.

M = momentum per sec = $(W/g)V$.

n = number of samples with $r < R$.

$\bar{n}$ = number of samples with $r > R$.

n' = total number of points sampled.

ΔP = pressure drop across orifice.

r = local mixture ratio = $w_2/(w_1 + w_2)$.

$\bar{r}$ = local mixture ratio for points where $r > R$.

r' = W_2/W_1.

R = nominal mixture ratio = $W_2/(W_1 + W_2)$.

t = time (sec).

U = maximum diameter of contour entry.

V = velocity (ft/sec).

w = total local weight flow rate of a spray.

W = total weight flow rate (lb/sec) or nominal weight flow rate of a spray.

W_d = weight of diluent added to sample (lb).

W_s = weight of sample (lb).

TABLE I (Cont'd)

Y = average value of the difference between local mixture ratio and nominal mixture ratio.

Y' = weighted average value of ratio of difference between local mixture ratio and nominal mixture ratio as a fraction of the nominal value.

Y'' = average and weighted value of departure of spray from nominal mixture ratio.

α = impingement angle; total angle included between stream center lines.

γ = angle between bisector of stream center lines and resultant momentum line of spray; taken to be positive for clockwise rotation of stream bisector.

δ = weight density of liquid (lb/cu ft).

ϵ = roughness factor = radius/magnitude of surface projection.

θ = angle of rotation of collector about the resultant momentum line from an arbitrary reference position taken as zero when the B-D axis is aligned in the plane of the stream center lines.

Subscripts

1 = first component of a spray (simulating a fuel).

2 = second component of a spray (simulating an oxidizer).

TABLE II

ORIFICE INSERTS USED TO STUDY LIQUID-PHASE MIXING
OF A PAIR OF IMPINGING STREAMS
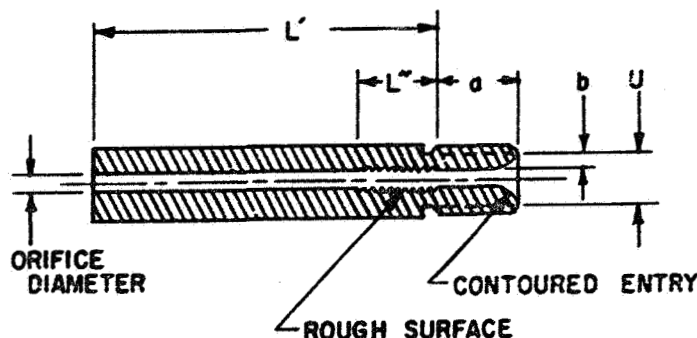
General Specifications

Orifice Diameter (in.)	Area (sq in. $\times 10^4$)	Area Scale Factor	For Radial[a] Contour			For Elliptical[b] Contour			
			$2a/D$	U	Orifice Identification No.[c]	$2a/D$	$2b/D$	U	Orifice Identification No.[c]
0.0400	12.56	1.0	5.69	0.275	9				
0.0529	21.98	1.75	4.53	0.287	10	9.61	2.40	0.177	1
0.0635	31.40	2.50	3.71	0.299	11	7.87	1.97	0.188	2
0.0785	47.20	3.75	3.00	0.314	12	6.36	1.59	0.203	3
0.0890	62.80	5.00				5.62	1.41	0.214	4
0.1093	94.30	7.50				4.57	1.14	0.234	5
0.1250	125.6	10.0				4.00	1.00	0.250	6

Test Orifices

Orifice No.	L'/D (straight)	ϵ[d]	Roughening Technique	L''/D (rough)
2A[e]	3.0	unknown	machined surface	none
9A, 9B	8.0			
9E-T, 9F-T, 9G-T, 9H-T	22.0	6.6	0.0460 by 80-thread tap	6.2
10E-T, 10F-T, 10G-T, 10H-T	22.0	6.5	No. 0-80 tap	6.0
11B	5.0	unknown	machined surface	none
11E-T, 11F-T	22.0	6.3	0.0732 by 80-thread tap	3.5
12C-T, 12D-T	22.0	3.4	No. 3-56 tap	3.5
12E-T, 12F-T	22.0	6.5	0.0905 by 80-thread tap	0.14

[a]Contour is constant for all diameters based on minimum radius of $1.5 \times D$ for a 0.125-in.-diameter orifice.

[b]Contour is constant for all diameters based on an ellipse with $2a/D=4.0$ and $2b/D=1.0$ for a 0.125-in.-diameter orifice.

[c]The number in this column is assigned to orifices incorporating the associated dimensions.

[d]Surface-roughness factor ϵ is equal to radius divided by magnitude of surface projection.

[e]Letter following orifice identification number denotes successive orifices having same diameter and entry contour.

[f]Letter T appended to orifice identification number signifies that the surface was roughened by tapping.

TABLE III
CONFIGURATION CONSTANTS AND SUMMARY OF RESULTS

Samples[a]	Orifice Subscript 1	Orifice Subscript 2	$\frac{M_1}{M_2}$	$\frac{A_1}{A_2}$	α (°)	γ[b]	R	Δp_1 (psi)	C_{d_1}	Δp_2 (psi)	C_{d_2}	$\frac{\Sigma C_w}{W}$	$\Sigma(KE)_x$	E_m	Remarks
62-71	10E-T	10E-T	1.0	1.0	60	variable	.558	100	.763	100	.767	1.16	0.9021	82.66	coordinate sampling; B-D axis deleted
72-77			1.0			0	.558	100	.763			1.17	0.9021	75.92	
79-84			1.0			0	.558	100	.763			1.18	0.9021	76.52	
78, 80-84			1.0			0	.558	100	.763			1.19	0.9021	75.73	samples 78 and 79 are similar
85-90			0.8		45	-3°40'	.585	80	.762			1.19	0.7318	74.15	
85-90			0.8		45	-3°40'	.585	80	.763			1.18	0.7318	74.37	
91-96			0.6		45	-8°18'	.620	60	.761			1.21	0.5869	66.45	
97-102			0.5		50	-10°53'	.661	50	.755			1.20	0.4876	65.91	
103-108			0.4			-15°54'	.666	40	.751			1.16	0.3903	59.92	
109-114			1.0			0	.558	100	.763			1.24	0.6905	80.75	
115-120			0.6		45	-5°54'	.620	60	.761			1.22	0.4490	75.47	
121-126			0.6		45	-5°54'	.620	60	.761			1.10	0.4490	65.93	
127-132			1.0		50	0	.558	100	.763			1.14	0.7634	78.13	
133-138			0.6		50	-6°38'	.620	60	.761			1.15	0.4952	66.53	
139-144			1.0		70	0	.558	100	.763			1.69	1.0348	73.54	
145-150			0.6		70	-9°55'	.620	60	.761			1.09	0.5868	60.18	
151-156			1.0		80	0	.558	100	.763			0.82	1.1397	70.63	
157-162			1.0		45	0	.553	100	.763			1.16	0.6905	79.89	
163-168			1.25		60	+8°40'	.531	100	.763	60	.766	1.07	0.7666	76.81	
169-174			1.67		60	+8°18'	.495	100	.763	60	.762	1.04	0.5993	68.75	

[a] Unless otherwise specified, $L = 0.5$ in., and the sprayed liquids are dyed water (subscript 1) and CCl_4 (subscript 2).

[b] The sign of γ is positive when the bisector of the stream center lines is rotated clockwise and when stream 1 is on the left and stream 2 on the right.

TABLE III (Cont'd)

Samples[a]	Orifice Subscript 1	Orifice Subscript 2	$\frac{W_1}{W_2}$	$\frac{A_1}{A_2}$	α (°)	γ	R	ΔP_1 (psi)	C_{d_1}	ΔP_2 (psi)	C_{d_2}	$\frac{\Sigma C \omega}{W}$	$\Sigma(\Delta E)_x$	δ_m	Remarks
213-218	9E-T	9F-T	1.0	1.0	60	0	.558	100	.764	100		0.90	0.5328	75.02	
219-224			0.6		60	−8°13'	.620	60	.769	100		0.90	0.3539	68.42	
225-231			1.67		60	+8°13'	.495	100	.764	60		1.06	0.3571	65.09	
232-237			1.0		45	0	.558	100	.764	100		0.95	0.4078	76.56	
238-243			1.0		70	0	.558	100	.764	100		0.88	0.6113	71.36	
244-249	11E-T	11F-T	1.0		60	0	.558	100	.795	100		1.09	1.5123	79.95	
250-255			0.6		60	−8°13'	.620	60	.790	100		1.12	0.9649	66.09	
256-261			1.67		60	+8°13'	.495	100	.795	60		1.03	1.0133	66.64	
262-267			1.0		45	0	.558	100	.795	100		1.19	1.1575	81.82	
268-273			1.0		70	0	.558	100	.795	100		0.74	1.7350	71.18	
273-279	12C-T	12D-T	1.0		60	0	.558	100	.787	100		1.11	2.2427	81.23	
280-285			0.6		60	+8°13'	.620	60	.788	100		1.10	1.6282	69.98	
286-291			1.67		60	−8°13'	.495	100	.787	60		1.01	1.8920	66.10	
292-297			1.0		45	0	.558	100	.787	100		1.18	1.7165	84.20	
298-303			1.0		70	0	.558	100	.787	100		0.99	2.5728	77.04	
314-319	10E-T	11E-T	1.04	0.670	60	0	.602	100	=C_{d_2}	64.5	.762	1.393	0.8344	83.33	
322-327			1.0			0	.606	100	.762	62.5	.789	1.311	0.8207	82.36	
328-333			0.8			−3°40'	.633	100	.762	78.0	.790	1.488	0.9530	85.10	
334-339			0.63			−8°13'	.661	97.8	.761	100	.795	1.575	1.0896	78.50	
340-345			0.4			−18°54'	.711	64.0	.761	100	.795	1.229	0.7237	62.31	
346-351			1.25			+5°40'	.580	100	.763	51.2	.781	2.437	0.6992	77.81	
352-357			1.67			+8°13'	.547	100	.762	39.8	.776	1.141	0.5637	66.83	
358-363			1.0		45	0	.606	100	.762	62.5	.789	1.250	0.6282	83.63	

C_{d_1} and C_{d_2} treated as equally less than 0.5% difference between

no sample for $\theta = 0°$

[a] Unless otherwise specified, $L = 0.5$ in., and the sprayed liquids are dyed water (subscript 1) and CCl_4 (subscript 2).

[b] The sign of γ is positive when the bisector of the stream center lines is rotated clockwise and when stream 1 is on the left and stream 2 on the right.

TABLE III (Cont'd)

| Samples[a]	Orifice Subscript 1	Orifice Subscript 2	$\frac{M_1}{M_2}$	$\frac{A_1}{A_2}$	α (°)	γ	R	ΔP_1 (psi)	C_{d_1}	ΔP_2 (psi)	C_{d_2}	$\frac{\Sigma C_d}{N}$	$\Sigma(KE)_x$	E_m	Remarks
364-369	10E-T	11E-T	1.67	0.670	45	+6°18'	.547	100	.762	39.5	.776	1.194	0.6051	66.16	
370-375		11E-T	0.6	0.670	45	-6°18'	.665	97.8	.761	100	.795	0.9566	0.8199	70.77	
376-381		11E-T	1.0	0.670	70	0	.606	100	.762	62.5	.780	0.9976	0.9416	80.17	
382-387		11E-T	0.6	0.670	70	-6°18'	.665	97.8	.761	100	.781	0.9081	1.2593	79.08	
392-397		12D-T	1.0	0.489	60	0	.658	100	.762	35.1	.776	1.134	0.7668	71.04	
398-403			1.67	0.489	60	+6°18'	.591	100	.762	71.2	.785	1.166	0.5193	45.49	
404-409			0.6	0.489	60	-6°18'	.713	100	.762	43.1	.781	1.361	1.0480	80.51	
410-415			1.0	0.489	45	0	.656	100	.762	25.5	.776	1.332	0.9189	63.81	
416-421				0.261	60		.712	100	.760	39.1	.769	1.390	0.6119	57.48	
422-427	9F-T	11E-T		0.397			.667	100	.769	60	.775	1.500	0.6390	77.10	
429-434	9G-T	10F-T		0.392			.621	100	.760	60	.753	0.9180	0.4596	77.72	
435-440	10F-T	9G-T		1.49			.692	99.2	.762	100	.781	0.9948	0.6783	63.89	
442-447	11E-T	12D-T		0.688			.609	100	.761	62.3	.750	1.329	1.1793	76.19	
480-485	10E-T	10F-T		1.0			.536	100	.762	100	.782	0.9076	0.6322	74.37	check for duplication of E_m
494-499	10G-T	10J-T					.551	100	.729	100	.775	0.9591	0.9890	75.97	orifice 10J-T rotated 90° clockwise from reference position
500-505	10G-T	10J-T					.551	100	.769	100	.775	0.9821	0.9890	73.61	both orifices at reference position
506-511	10J-T	10G-T					.551	100	.775	95	.799	0.9803	0.9516	76.35	interchanged orifices

[a] Unless otherwise specified, L = 0.5 in., and the sprayed liquids are dyed water (subscript 1) and CCl_4 (subscript 2).

[b] The sign of γ is positive when the bisector of the stream center lines is rotated clockwise and when stream 1 is on the left and stream 2 on the right.

TABLE III (Cont'd)

Samples[a]	Orifice Subscript 1	Subscript 2	$\frac{M_3}{M_2}$	$\frac{A_1}{A_2}$	α (°)	γ[b]	R	ΔP_1 (psi)	C_{d_1}	ΔP_2 (psi)	C_{d_2}	$\frac{\Sigma \Gamma \omega}{\Delta V}$	$\Sigma(\Delta E)_x$	E_m	Remarks
512-517	10E-T	10F-T	1.0	1.0	60	0	.474	100	.765[d]	100	.760[d]	0.9343	1.0213	76.96	substituted kerosene for CCl₄
512-516, 517L	10E-T	10F-T				0	.474	–	.766	–	.764	0.9343	1.0213	77.75	517L is 517 after 2-hr settling period
518-523	10F-T	10E-T				+2°20'	.466	–	.765[d]	–	.751[d]	0.8028	1.0600	76.50	reversed orifices with system H₂O-kerosene
524-529	10F-T	10F-T				0	.558	–	.762	100	.762	0.9032	0.8922	74.87	$L = 0.5$ in.
530-535							.558	100	.762	100	.762	0.9360	0.8922	73.91	$L = 0.75$ in.
536-541							.559	25	.745	25	.744	0.857?	0.1041	70.78	$\Delta P_1 = \Delta P_2 = 25$ psi
542-547							.560	50	.755	50	.750	0.8680	0.8097	70.91	$\Delta P_1 = \Delta P_2 = 50$ psi
548-553							.562	200	.767	200	.777	0.9603	2.6183	78.09	$\Delta P_1 = \Delta P_2 = 200$ psi
554-559							.562	200	.767	200	.777	0.9398	2.6183	73.57	check on samples 548-553
560-565	10F-T	10E-T				-6°13' / +6°13'	.560	200	.768	200	.773	1.157	2.6065	81.75	same as samples 554-559 with reversed orifices
567-572	10E-T	10F-T					.500	100	.760	100	.762	1.146	0.9922	83.43	miscible liquids, H₂O and dyed H₂O
573-578	10E-T	10F-T	0.6				.564	60	.761	100	.762	1.109	0.6549	80.09	
579-584	10E-T	10F-T	1.67				.433	100	.760	60	.753	1.154	0.6433	79.18	

[a] Unless otherwise specified, $L = 0.5$ in., and the sprayed liquids are dyed water (subscript 1) and CCl₄ (subscript 2).

[b] The sign of γ is positive when the bisector of the stream center lines is rotated clockwise and when stream 1 is on the left and stream 2 on the right.

[c] Change in γ necessary to compensate for change in C_d with Reynolds number.

[d] Based on recalibration of May 5, 1952.

TABLE IV

AREA CORRECTION FACTORS FOR POLAR-SAMPLING AREAS[a]
WITH 15° INCREMENTS

$$A_s = \frac{\pi}{2}(c_2 - c_1)$$
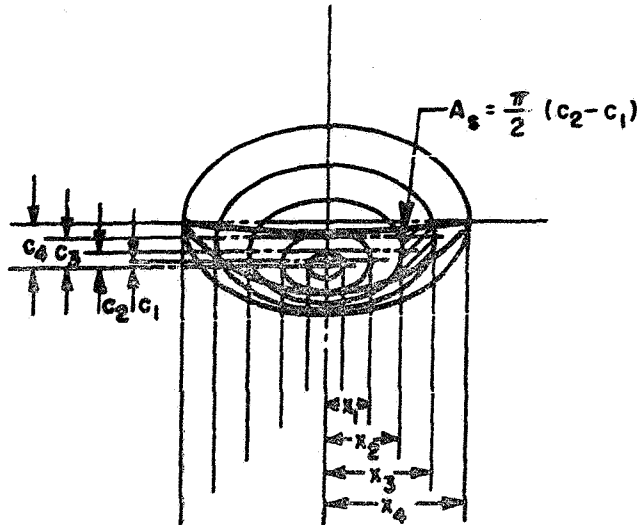
Tube No.	A_s/A_t	Tube No.	A_s/A_t
0	0.360	10	7.93
1	0.722	11	8.92
2	1.45	12	9.99
3	2.18	13	11.15
4	2.92	14	12.43
5	3.69	15	13.86
6	4.47	16	15.48
7	5.28	17	17.37
8	6.12	18	19.64
9	7.00		

[a]In this sketch, A_s is the sampling area, that portion of the area of a lune which has a dihedral angle of 15° and its axis coincident with the spray axis and which is bounded by the intersection of two cylindrical surfaces, the axes of which are coincident with the spray axis (radius x_1 of center cylinder = 0.125 in., and radii of successive cylinders x_2, x_3, etc. increase in ... increments). $A_s = (\pi/2)(c_2 - c_1)$ when the radius of the sphere equals 6 inches.

TABLE V

PHYSICAL PROPERTIES OF SPRAYED FLUIDS

Fluid	Dye Concentration (wt %)	Density at 20°C (gm/cc)	Viscosity at 20°C (centipoises)	Surface Tension at 20°C (dynes/cm)
Dyed water[a]	0.015	0.998	1.009	72.75
Dyed water[b]	0.1	0.998	1.009	72.75
Carbon tetrachloride[c]	none	1.592	0.975	26.8
Kerosene (white)[d]	none	0.810	1.90	28.0

[a]Dye concentration approximate since dye was added for photographic contrast only.

[b]Used for tests with miscible liquids.

[c]From Ref. 19.

[d]By JPL analytical laboratory on high-grade commercial product by Union Oil Co.

TABLE VI
TYPICAL DATA SHEET[a] FOR SAMPLE 322

Tube No.	h_2 (in.)	h (in.)	$h-h_2$ (in.)	$w_1 \times 10^5$	$w_2 \times 10^5$	$w_5 \times 10^5$	r	$R-r$	$C_w \times 10^5$	$C_w(R-r) \times 10^6$	$C_w(R-\bar{r}) \times 10^6$
0	1.07	3.00	1.93	158.2	140.0	298.2	0.469	0.137	1,074.0	147.1	
A-1	1.05	2.88	1.83	150.0	187.4	287.4	0.478	0.128	2,075.0	265.6	
A-2	1.00	2.77	1.77	145.1	130.8	275.9	0.474	0.132	4,001.0	528.1	
A-3	0.99	2.65	1.66	186.1	129.5	265.6	0.488	0.118	5,790.0	683.2	
A-4	1.00	2.59	1.59	130.8	130.8	261.1	0.501	0.105	7,624.0	800.5	
A-5	0.99	2.42	1.43	117.2	129.5	246.7	0.525	0.081	9,103.0	737.3	
A-6	1.05	2.41	1.36	111.5	137.4	248.9	0.552	0.054	11,126.0	600.8	
A-7	1.00	2.20	1.20	99.36	130.8	229.2	0.571	0.035	12,102.0	432.6	
A-8	1.03	2.20	1.17	95.90	134.8	230.7	0.584	0.022	14,119.0	310.6	
A-9	1.00	2.03	1.03	84.42	130.8	215.2	0.608	-0.002	15,066.0	--	30.13
A-10	0.93	1.83	0.90	78.77	121.7	195.5	0.623	-0.017	15,503.0	--	263.6
A-11	0.77	1.50	0.73	59.83	100.7	160.5	0.627	-0.021	14,317.0	--	300.7
A-12	0.62	1.17	0.55	45.08	81.11	126.2	0.643	-0.037	12,607.0	--	466.5
A-13	0.46	0.83	0.37	30.38	60.18	90.51	0.665	-0.059	10,092.0	--	595.4
A-14	0.33	0.67	0.34	27.87	43.17	71.04	0.608	-0.002	8,830.0	--	17.66
A-15	0.27	0.54	0.27	22.13	35.32	57.45	0.615	-0.009	7,963.0	--	71.67
A-16	0.15	0.35	0.20	16.39	19.62	36.01	0.545	0.061	5,574.0	340.0	
A-17	0.12	0.29	0.17	13.98	15.70	29.63	0.530	0.076	5,147.0	391.2	
A-18	0.06	0.20	0.14	11.48	7.850	19.33	0.406	0.200	3,796.0	759.2	
Total									165,907.0	5,987.2	1,745.66

[a]The following test conditions apply in this table: operating conditions with orifices 10E-T(H_2O) and 11E-T(CCl_4) where

$$\Delta P_1/P_2 = 1.60 = 100/62.5, \text{ and } (C_{d_1}/C_{d_2})^2 = 0.932 \text{ when } R = 0.606, M_1/M_2 = 1.0, \alpha = 60°, \text{ and } \theta = 0°.$$

TABLE VII

EXPERIMENTAL VARIATION[a] OF E_m

Sample No.	Orifice No.		Date Taken	E_m	Remarks
	H_2O	CCl_4			
72 through 77	10E-T	10F-T	4-4-51	75.92	original data taken to study effect of M_1/M_2
79 through 84	10E-T	10F-T	4-51	76.52	check on original data to establish experimental duplication
480 through 485	10E-T	10F-T	1-29-52	74.37	check on original data with duplicate configuration
500 through 505	10F-T	10J-T	3-5-52	73.61	check on original data with duplicate set of orifices
494 through 499	10G-T	10J-T	3-4-52	75.97	same as samples 500 through 505 except that orifice 10J-T was rotated 90° clockwise
506 through 511	10J-T	10G-T	3-6-52	76.85	same as samples 500 through 505 except for interchange of orifices
				Av 75.45	

[a] The following test conditions were constant for these data: $M_1/M_2 = 1.0$; $A_1/A_2 = 1.0$; $\alpha = 60°$; $\Delta P_1 = \Delta P_2 = 100$ psi; $D_1 = D_2 = 0.052$ in.; and $C_{d_1} = C_{d_2} = 0.766$.

TABLE VIII

VARIATION OF E_m WITH MOMENTUM RATIO FOR MISCIBLE LIQUIDS

M_1/M_2	A_1/A_2	α (°)	ΔP_1	ΔP_2	E_m
0.6	1.0	60	60	100	80.09
1.0	1.0	60	100	100	83.47
1.67	1.0	60	100	60	79.18
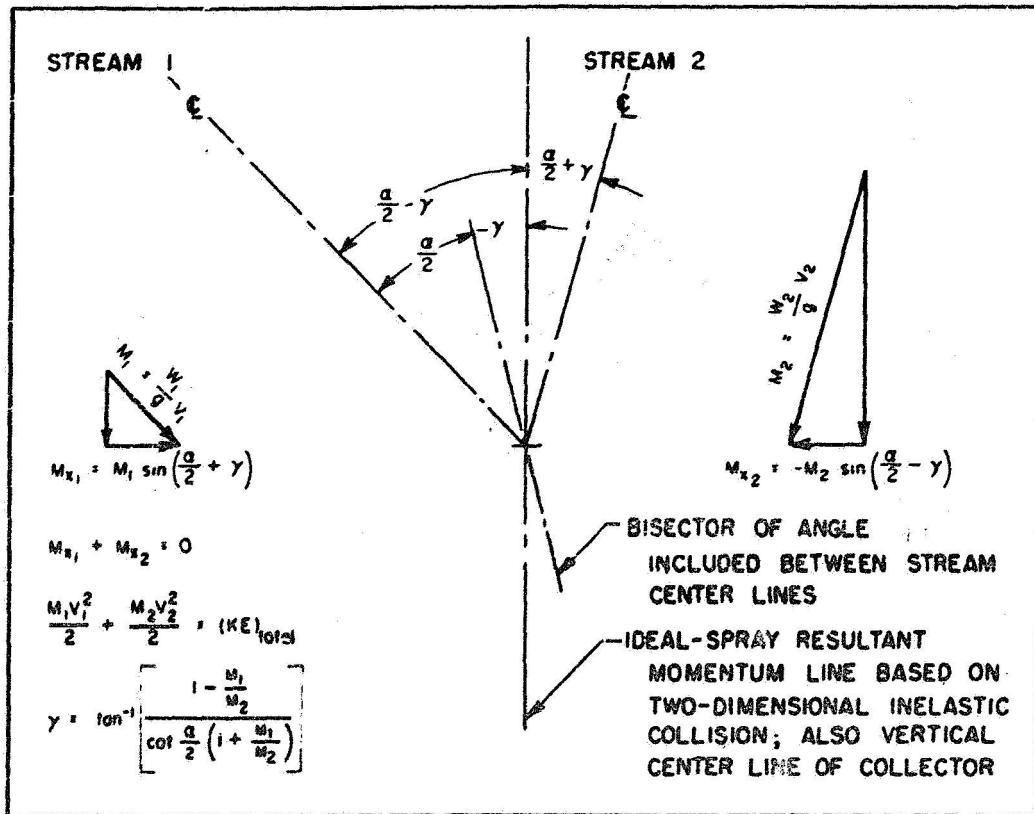
Figure 1.   Geometry of Impinging-Stream System
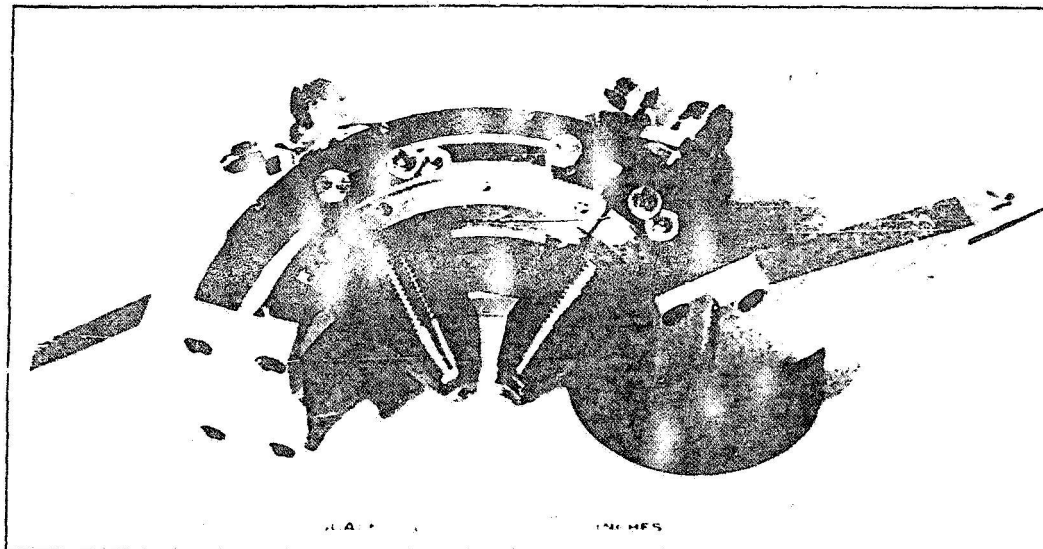
Figure 2.   Impinging-Jet Assembly
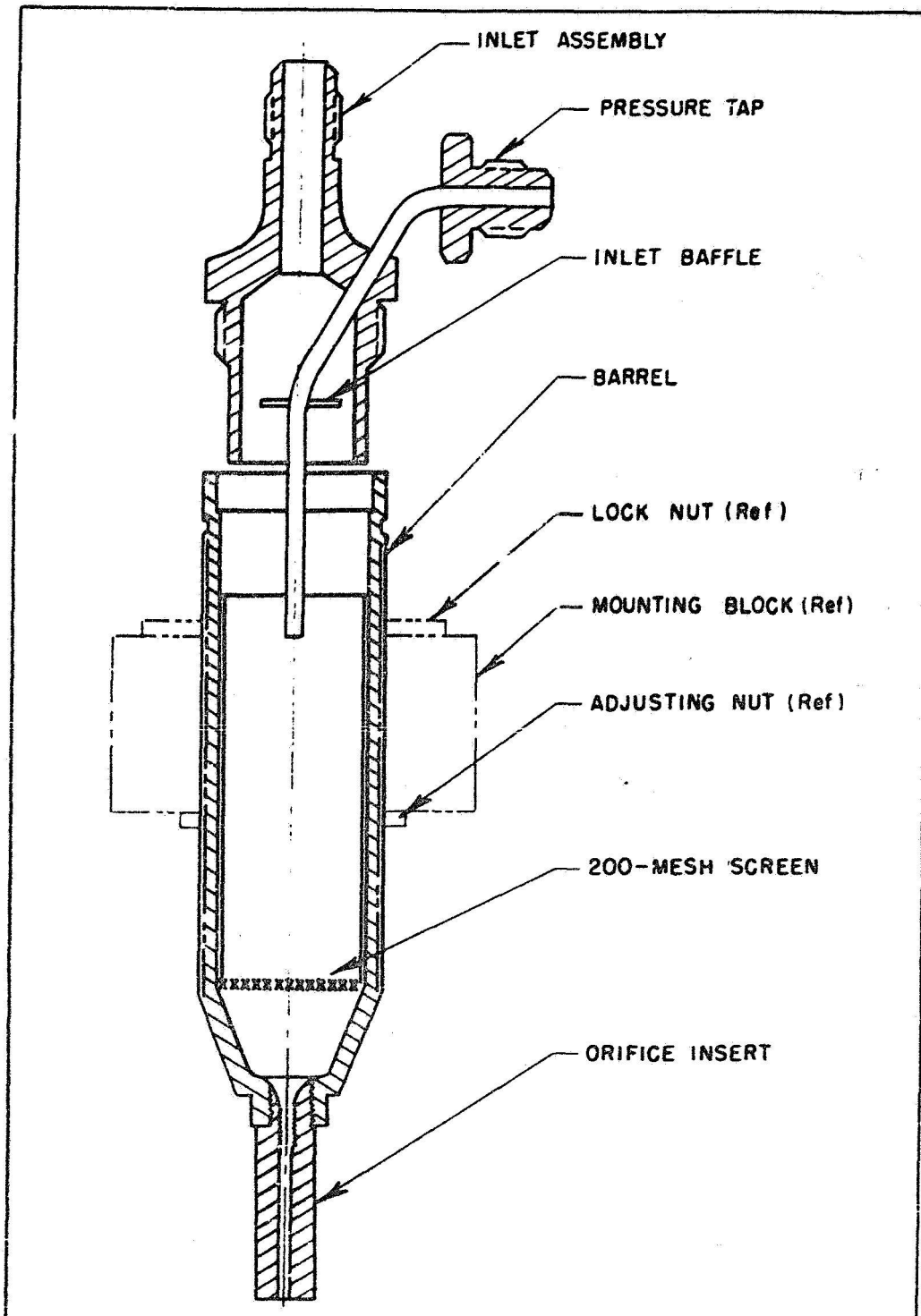
Figure 3.   Barrel Assembly
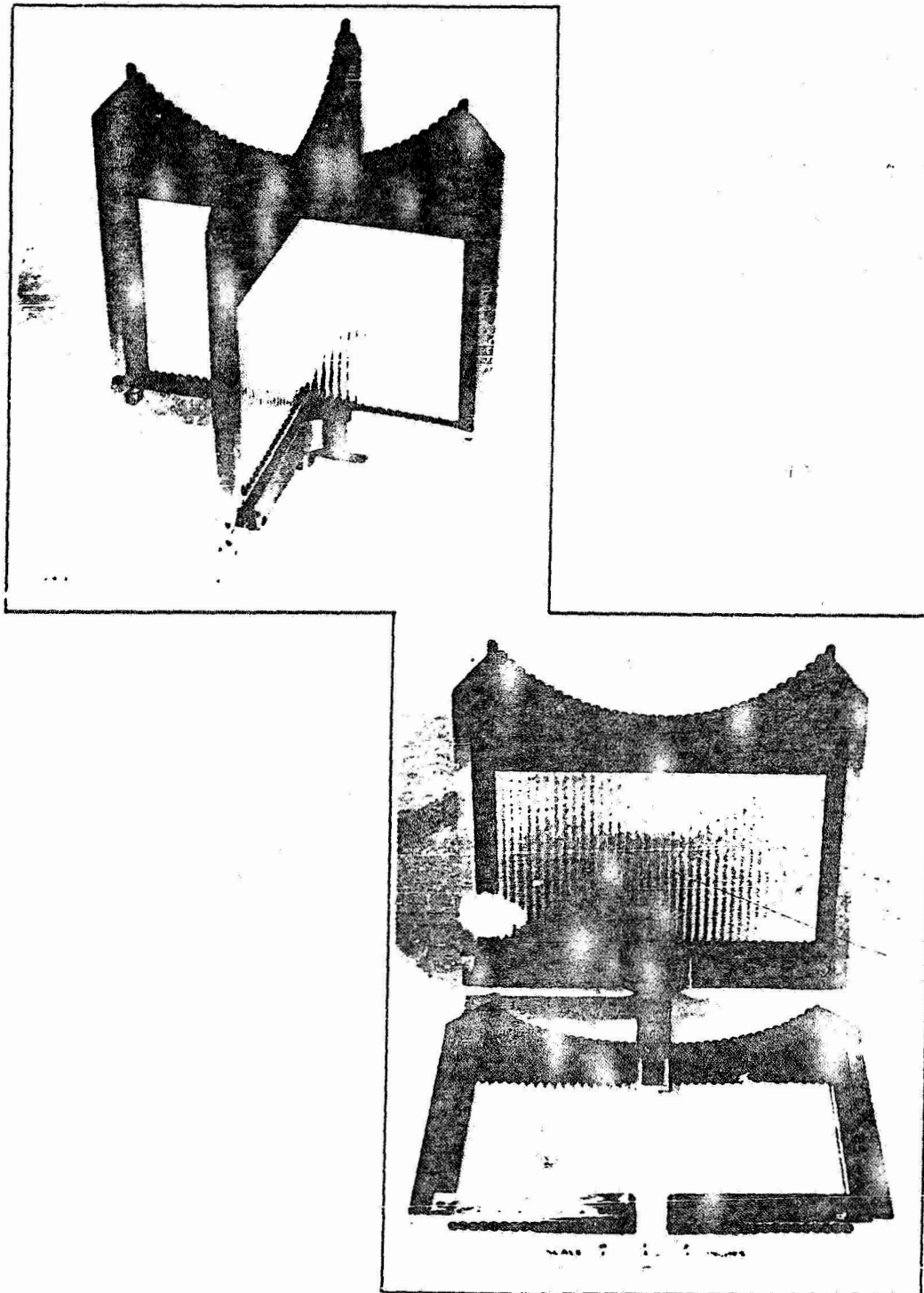
Figure 4.   Collector Assembly with 6-Inch Radius
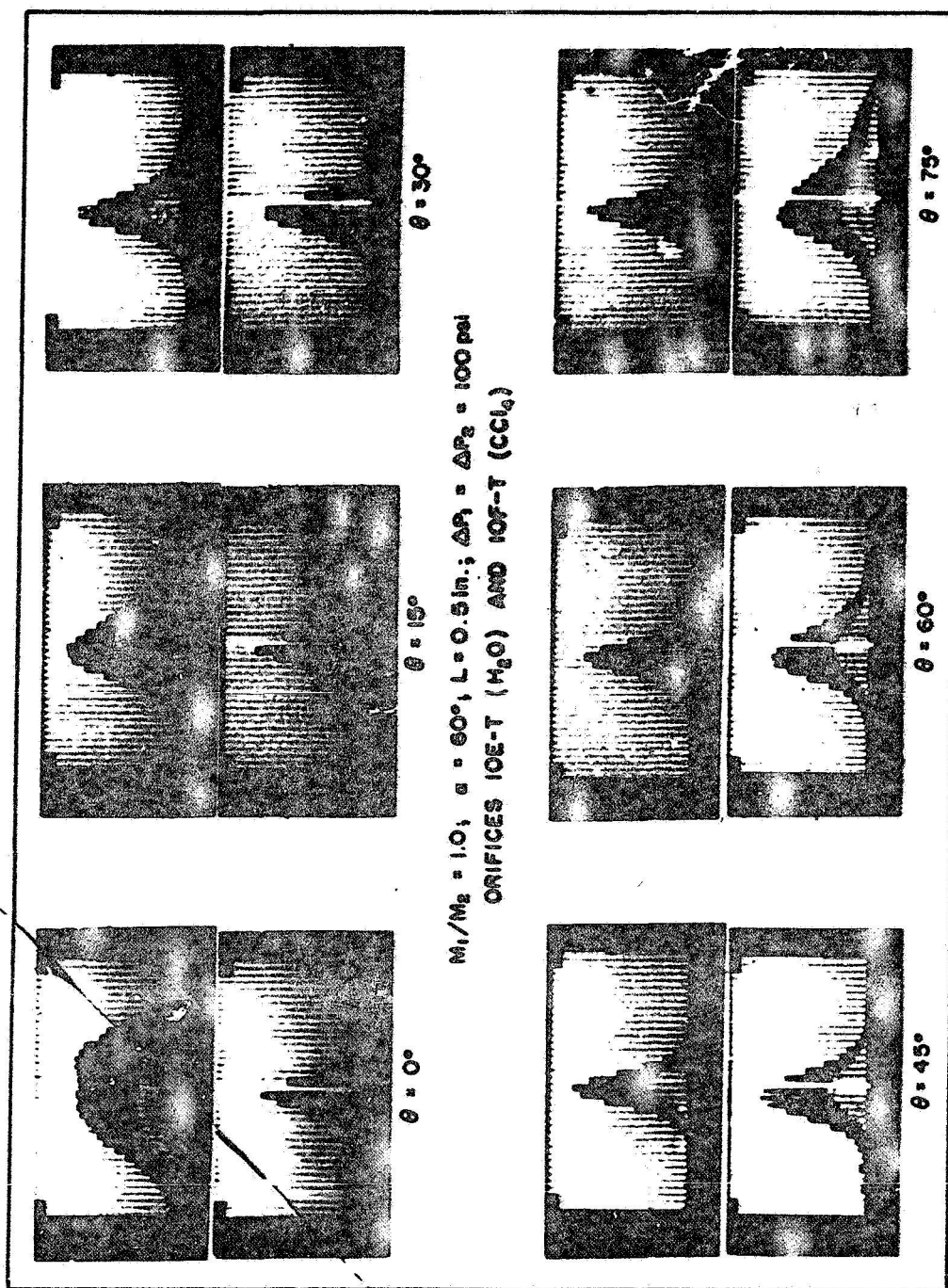
Figure 5. Variation of Spatial Distribution with Collector Position
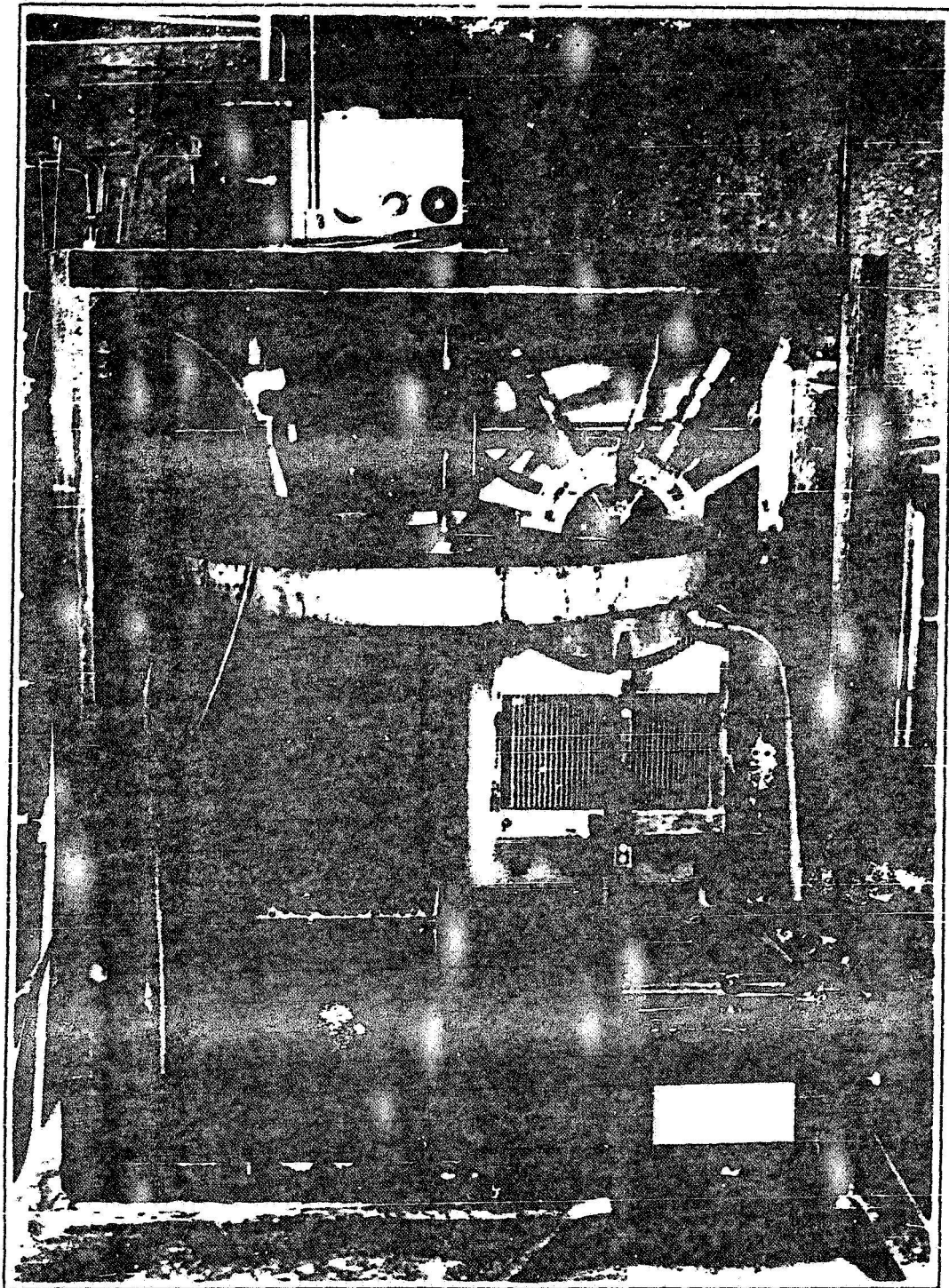
Figure 6.   Injector Spray Booth

ΔP = 25 psi

ΔP = 25 psi

ΔP = 100 psi

INJECTORS: IIB AND 2A
e = 60°
SYSTEM : WATER - WATER
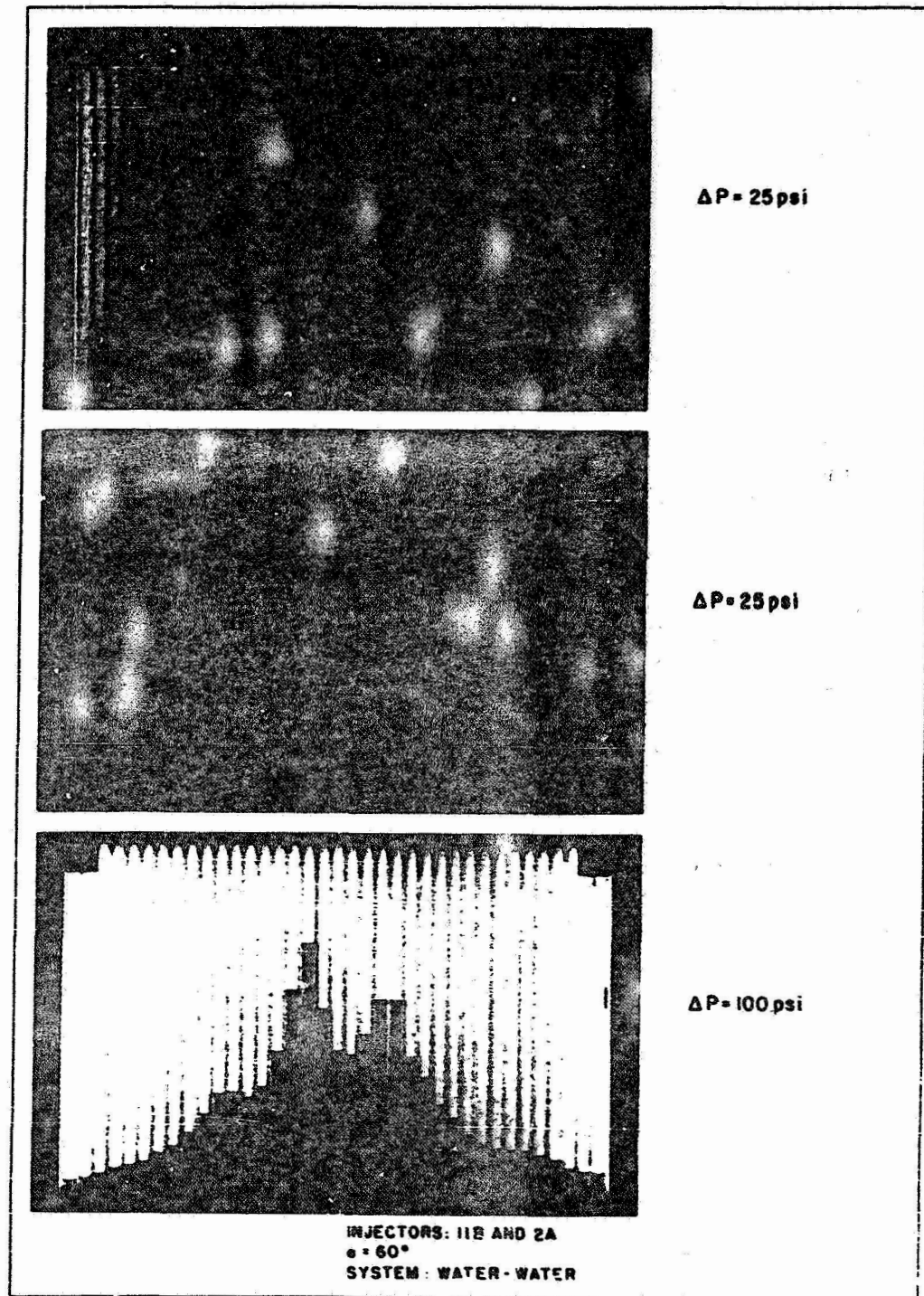
Figure 7.   Variation of Spatial Distribution Resulting from Poor Free-Stream Characteristics

INJECTORS: 9B AND 9A
$a = 60°$; $\Delta P = 25$ psi
SYSTEM : WATER - WATER
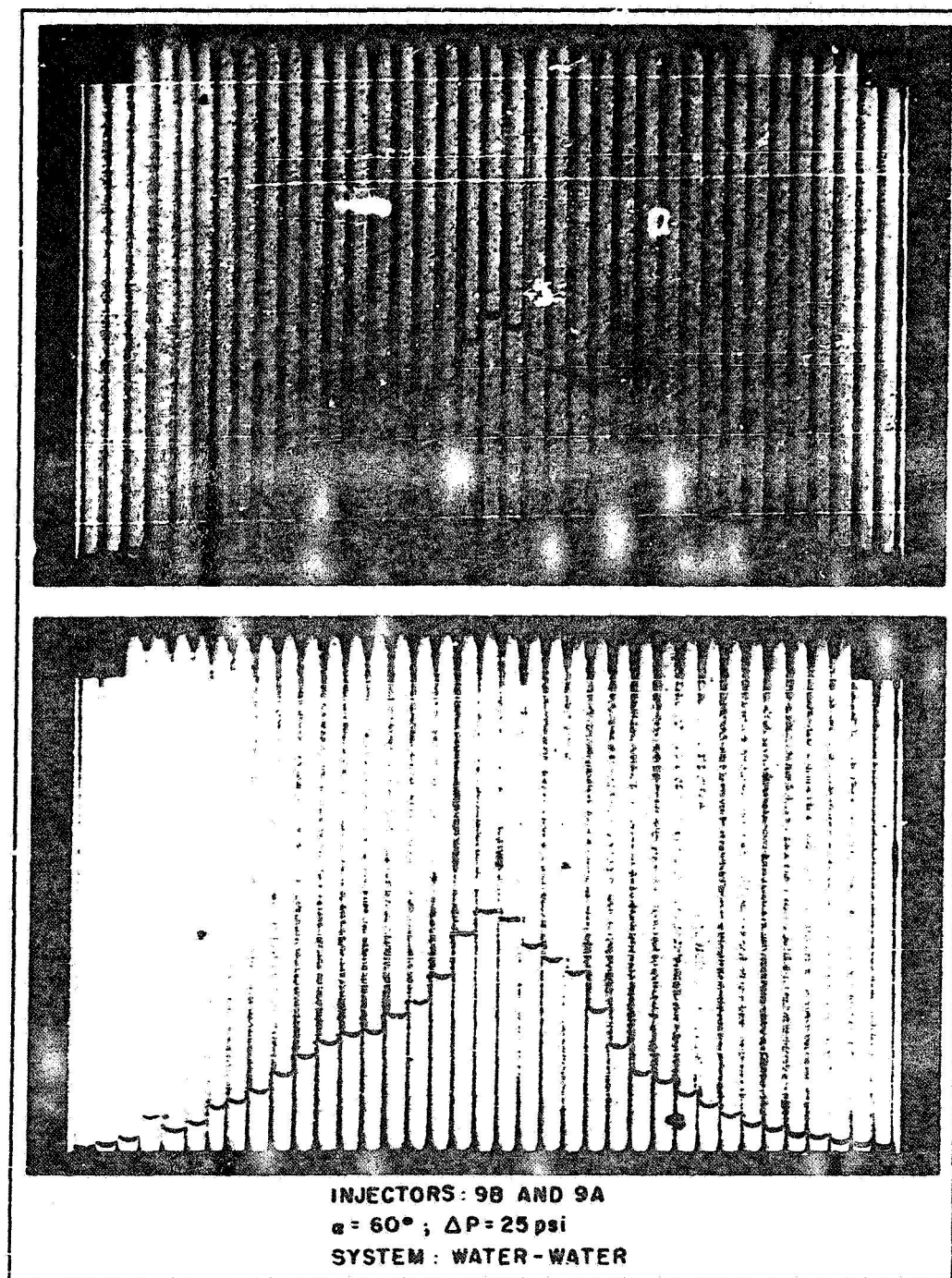
Figure 8.   Reproducibility in Spatial Distribution of Streams of Good Free-Stream Characteristics

BARREL 1 ROTATED 30° CLOCKWISE

BARREL 2 ROTATED 30° CLOCKWISE

BARREL ROTATED 60° CLOCKWISE

BARREL 2 ROTATED 60° CLOCKWISE

BARREL ROTATED 90° CLOCKWISE

BARREL 2 ROTATED 90° CLOCKWISE

INJECTORS 9B AND 9A
$\alpha = 60°$, $\Delta P = 50$ psi
SYSTEM WATER-WATER
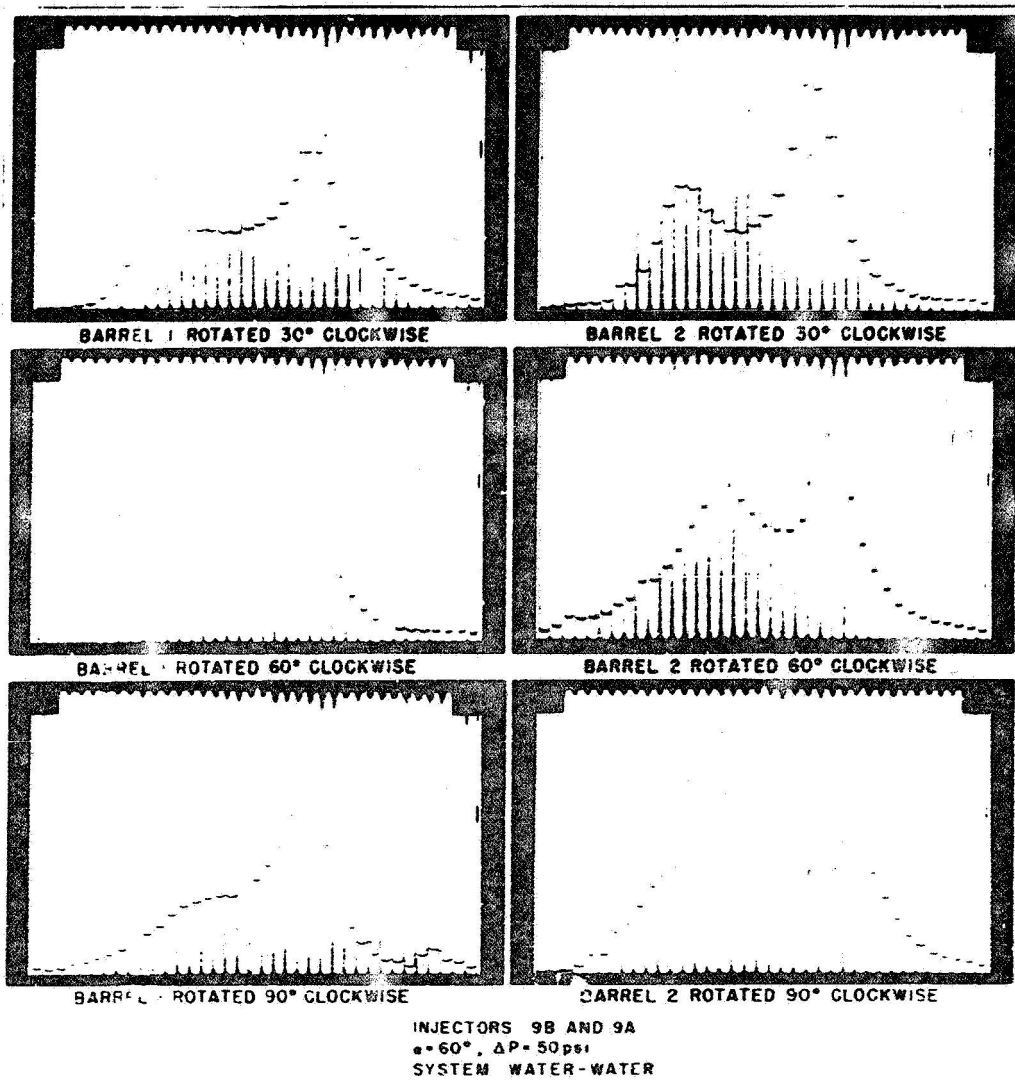
Figure 9. Variation in Spatial Distribution Resulting from Radial Displacement of Nonsymmetrical Velocity Profiles
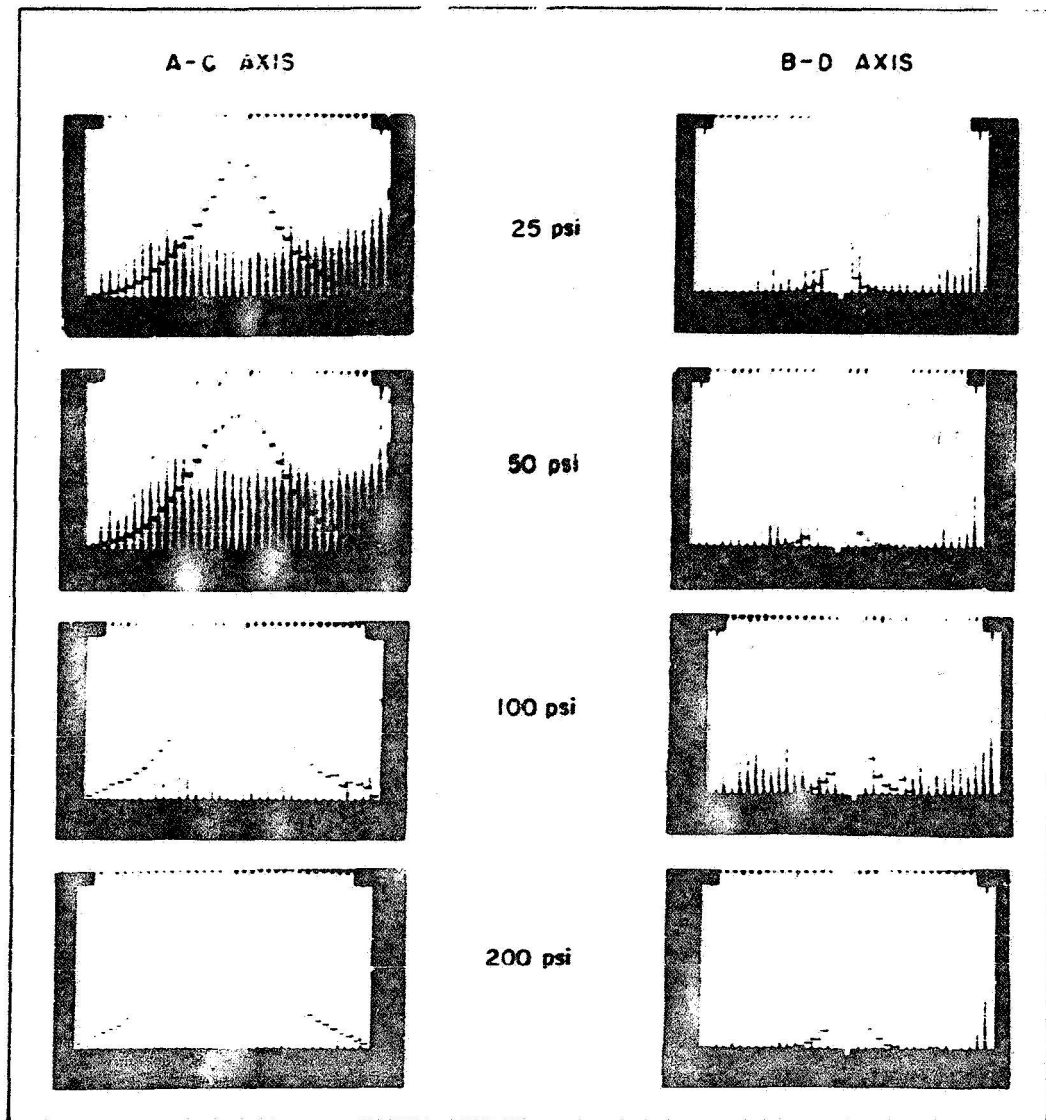
Figure 10.   Spatial Distribution from Streams with Symmetrical Velocity Profiles
at Various Reynolds Numbers
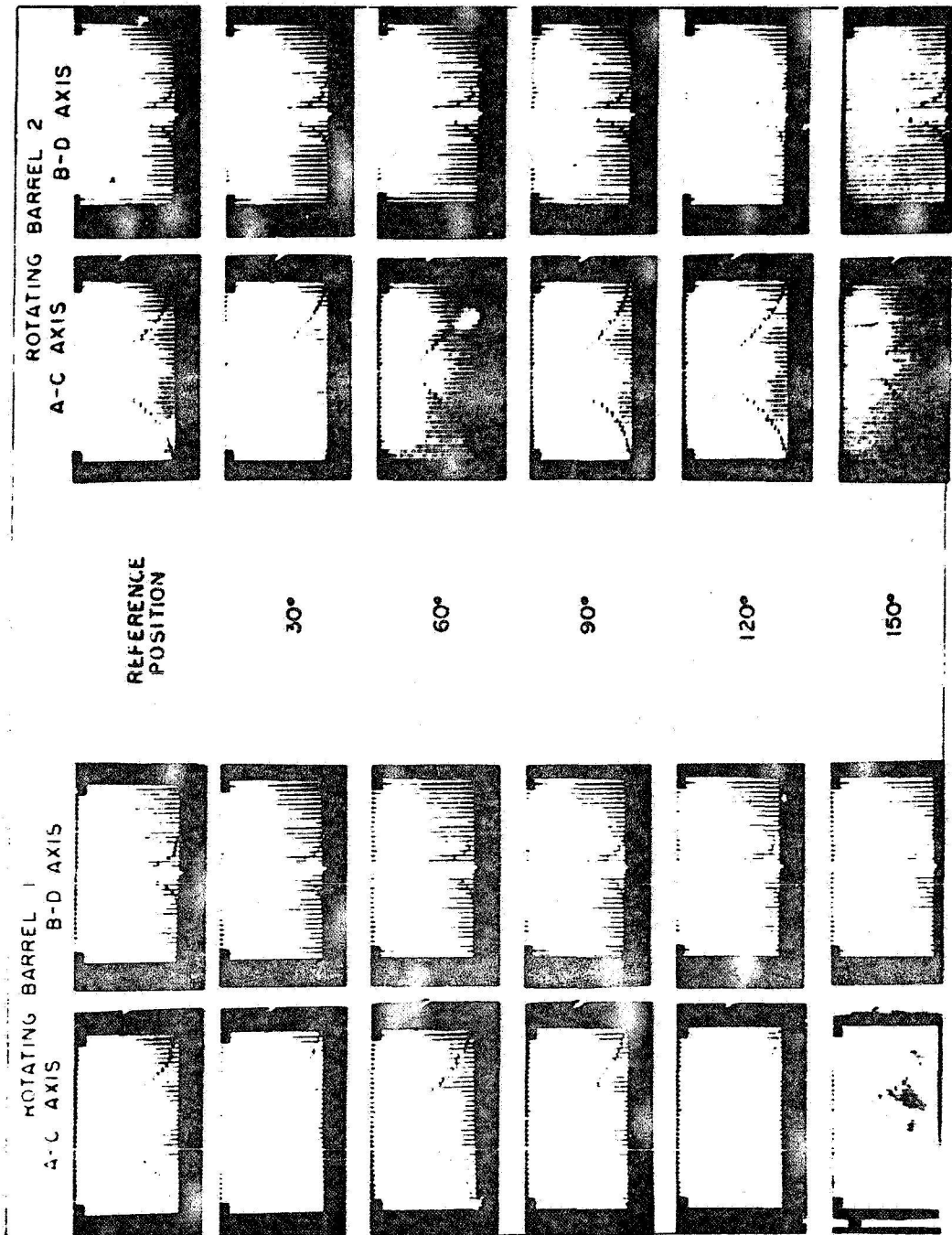
Figure 11.   Spatial Distribution from Streams with Symmetrical Velocity Profiles for Variation of Relative Impingement Position
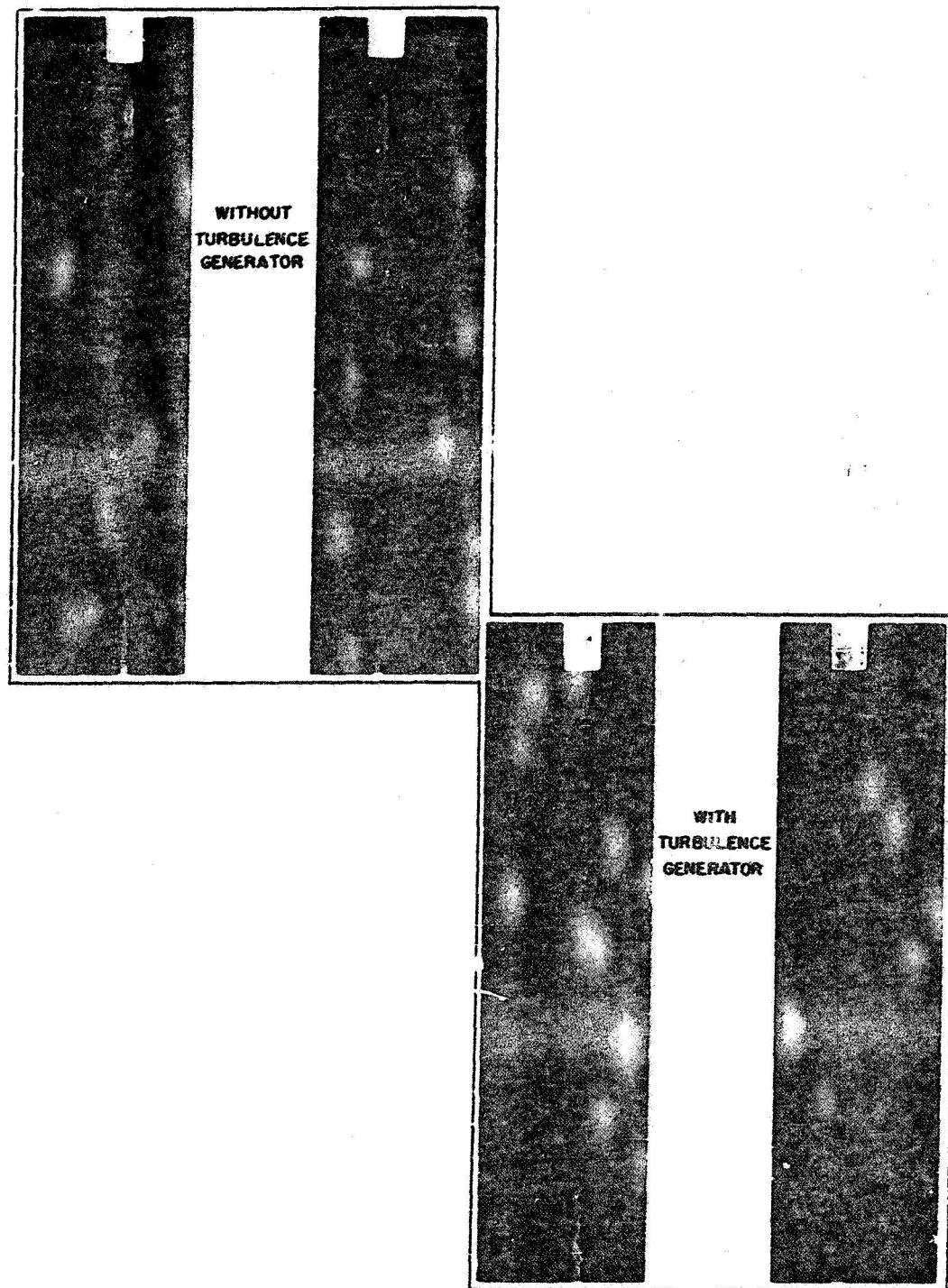
Figure 12.   Flash Photographs of Free Streams Without and With Turbulence Generator

A. MINOR AXIS

B. MAJOR AXIS
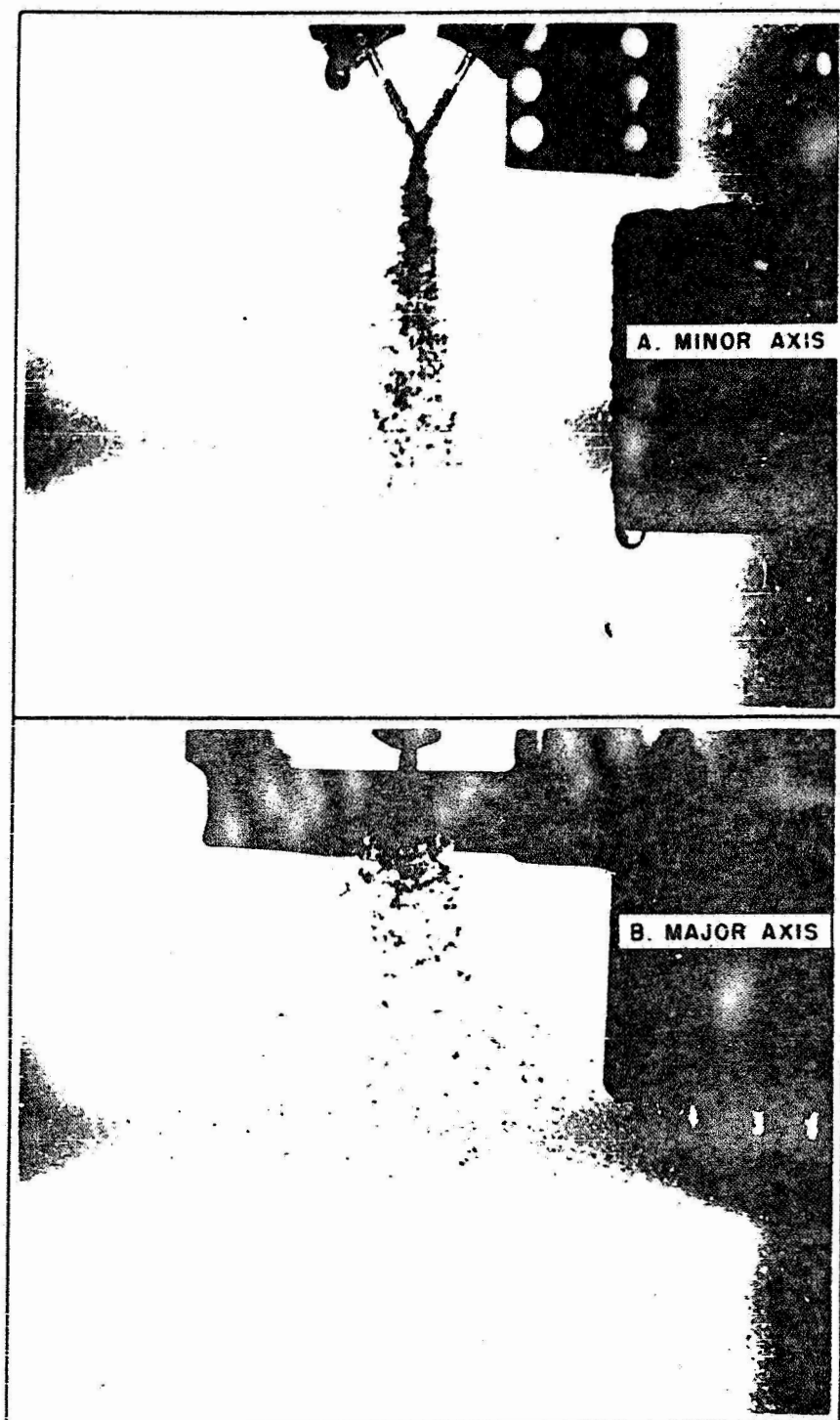
Figure 13. High-Speed Flash Photographs of Sprays Produced by Incipiently
Turbulent Streams
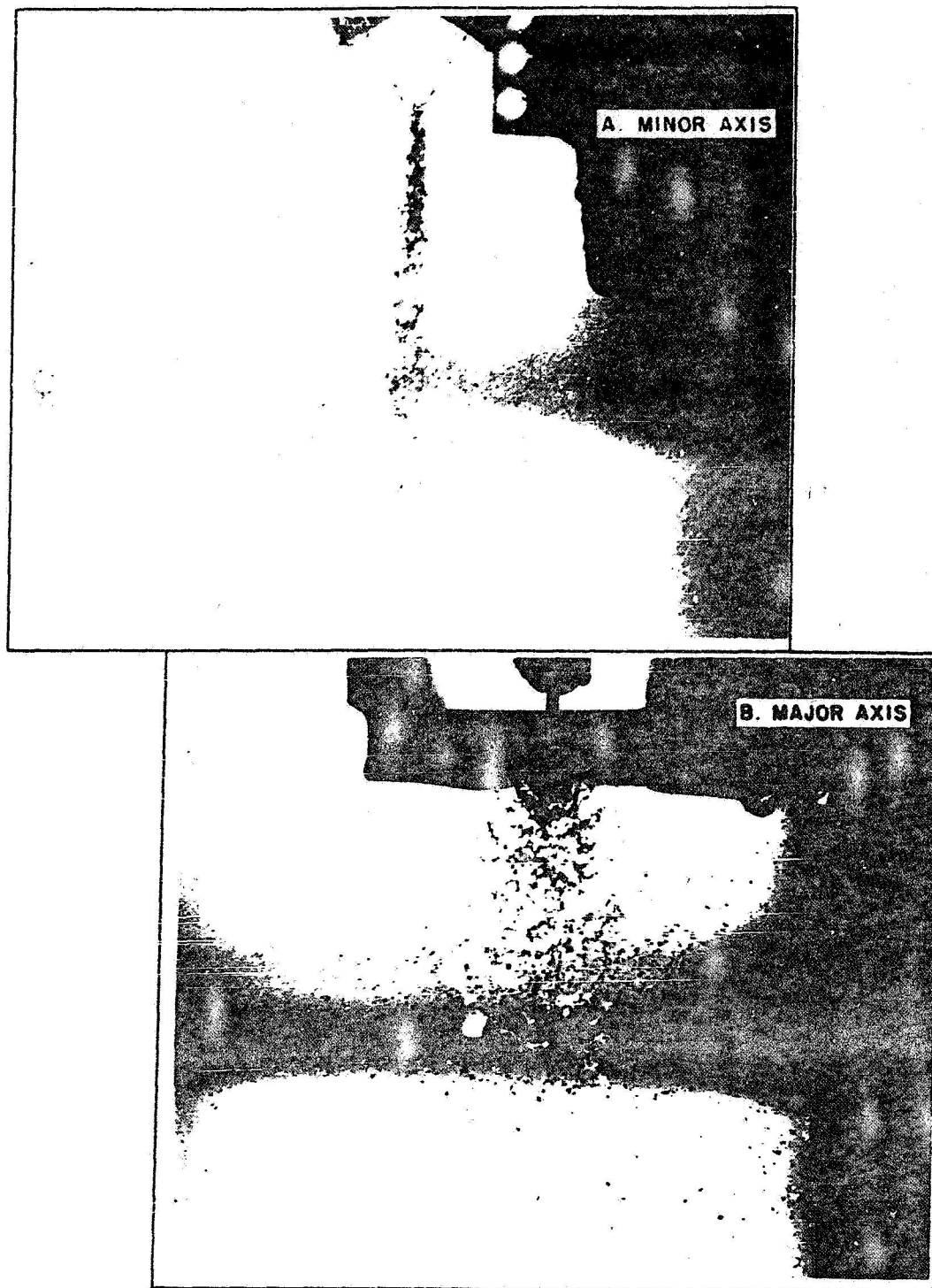
Figure 14.   High-Speed Flash Photographs of Sprays Produced by Fully Turbulent Streams
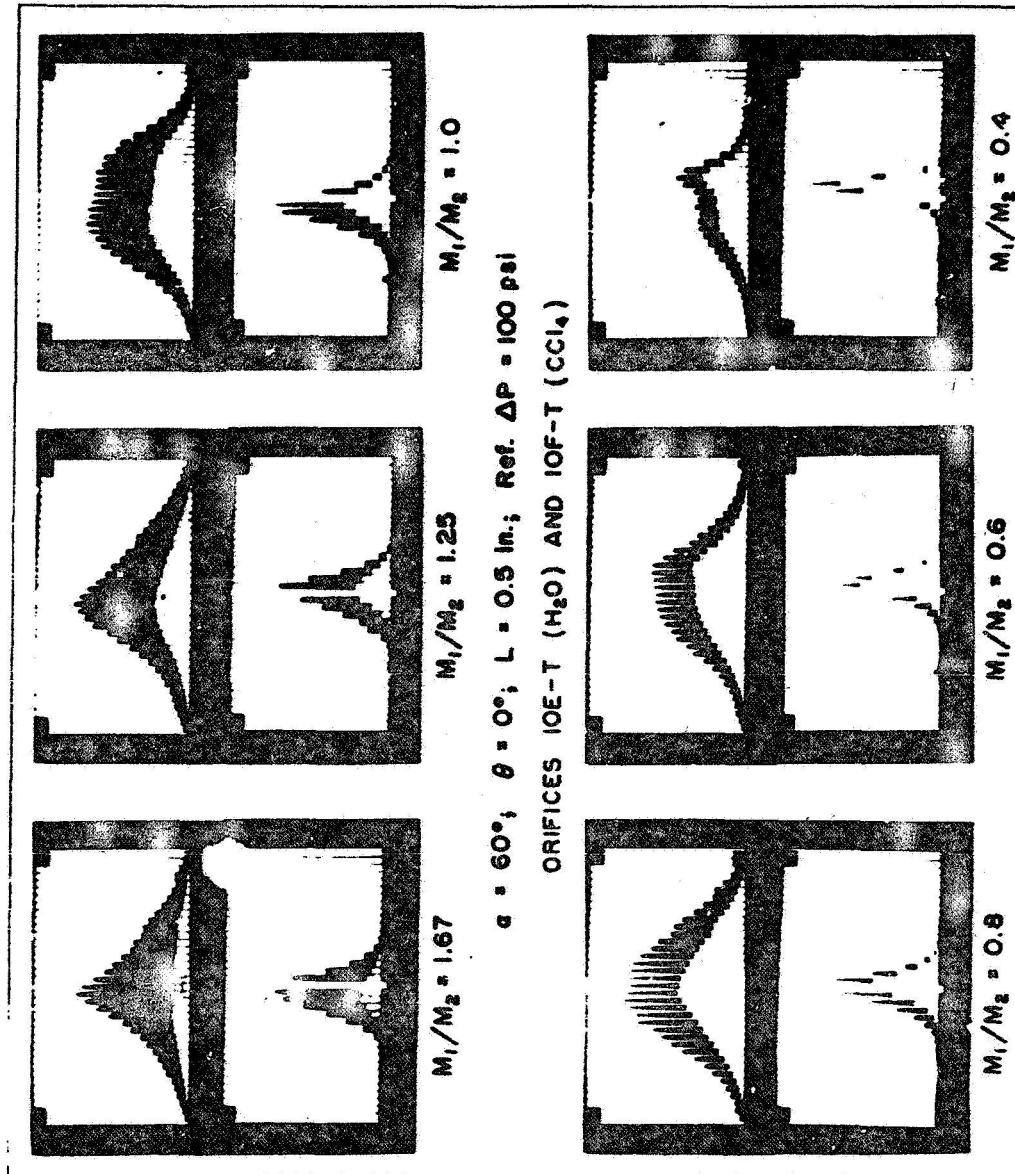
Figure 15.   Variation of Spatial Distribution with Momentum Ratio

$M_1/M_2 = 1.0$; $\Delta P_1 = \Delta P_2 = 100$ psi; $\theta = 0°$; $L = 0.5$ in.

ORIFICES IOE-T (H_2O) AND IOF-T (CCl_4)
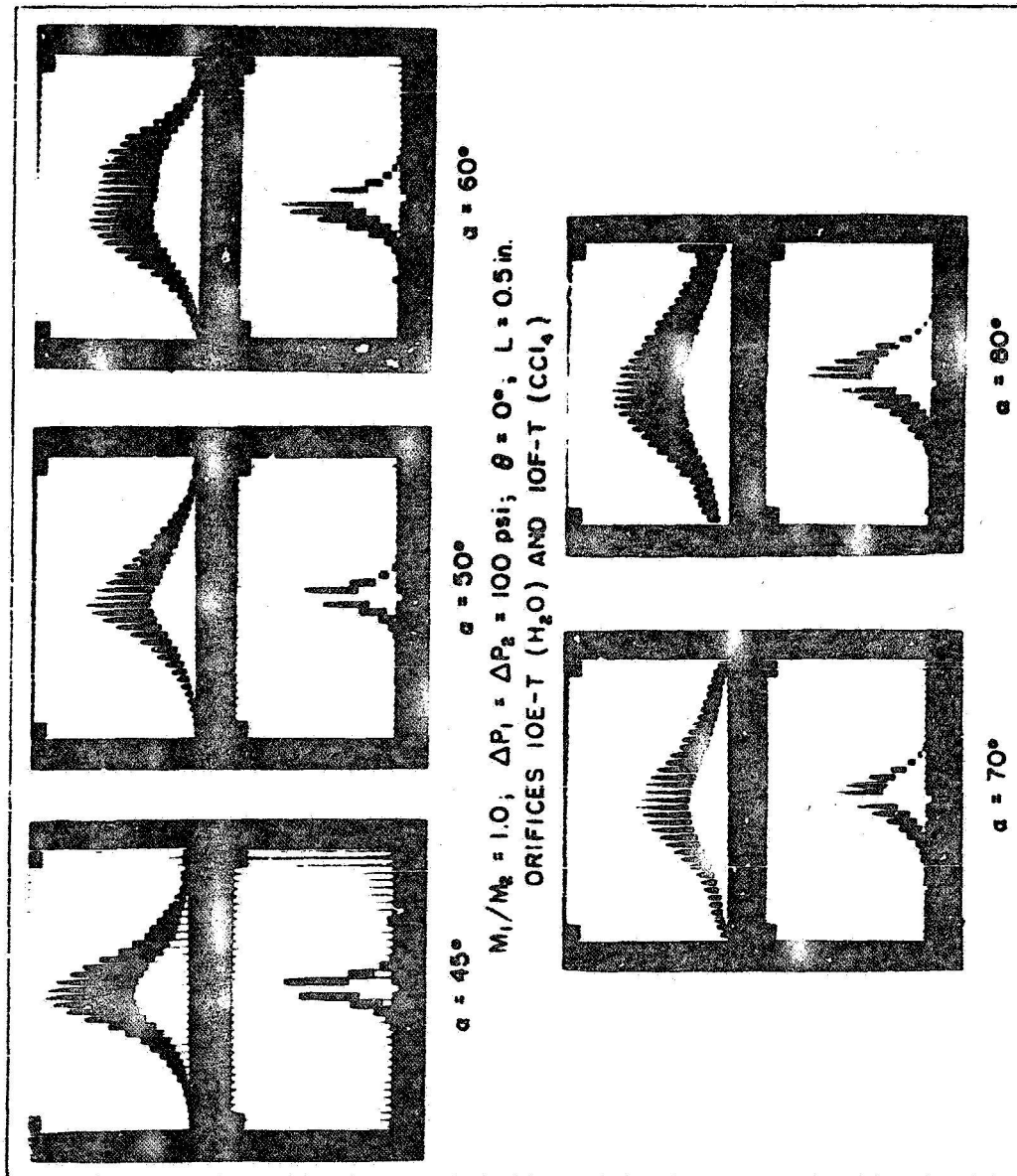
Figure 16. Variation of Spatial Distribution with Impingement Angle
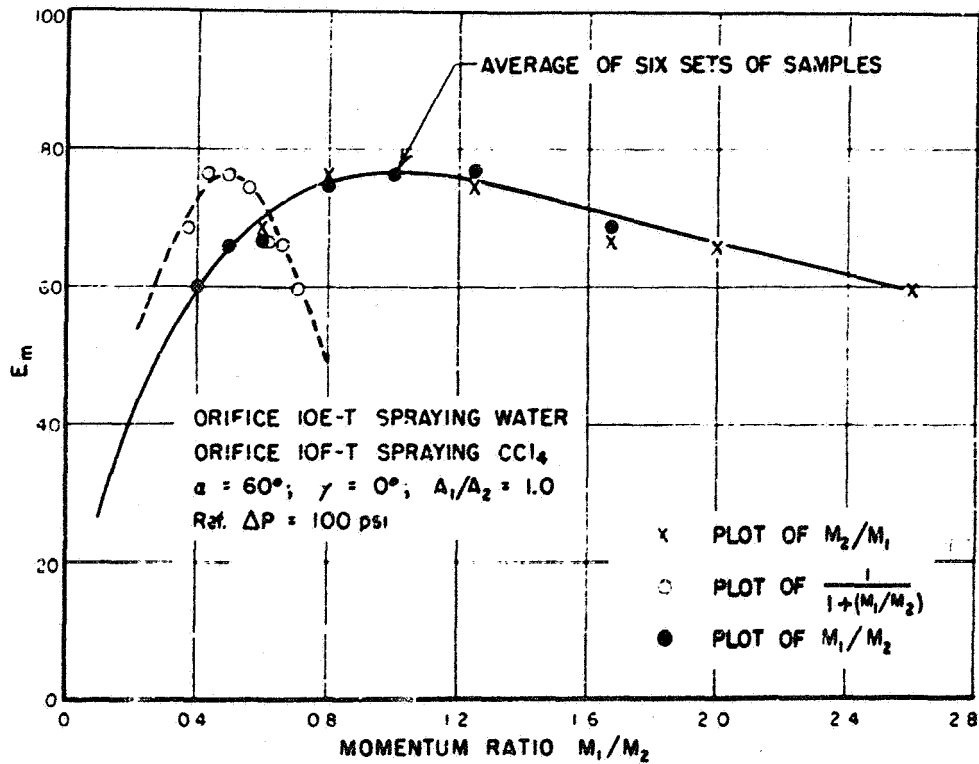
Figure 17.   Variation of E_m with M_1 M_2
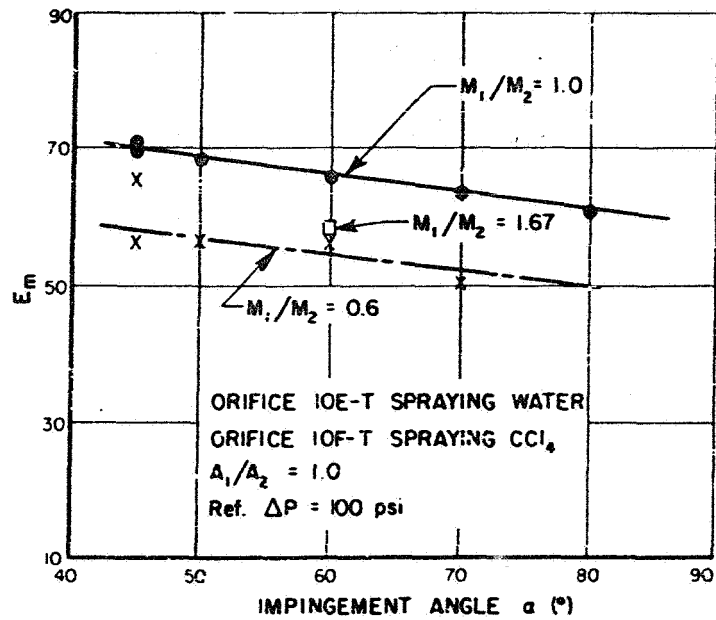
Figure 18.   Variation of E_m with α
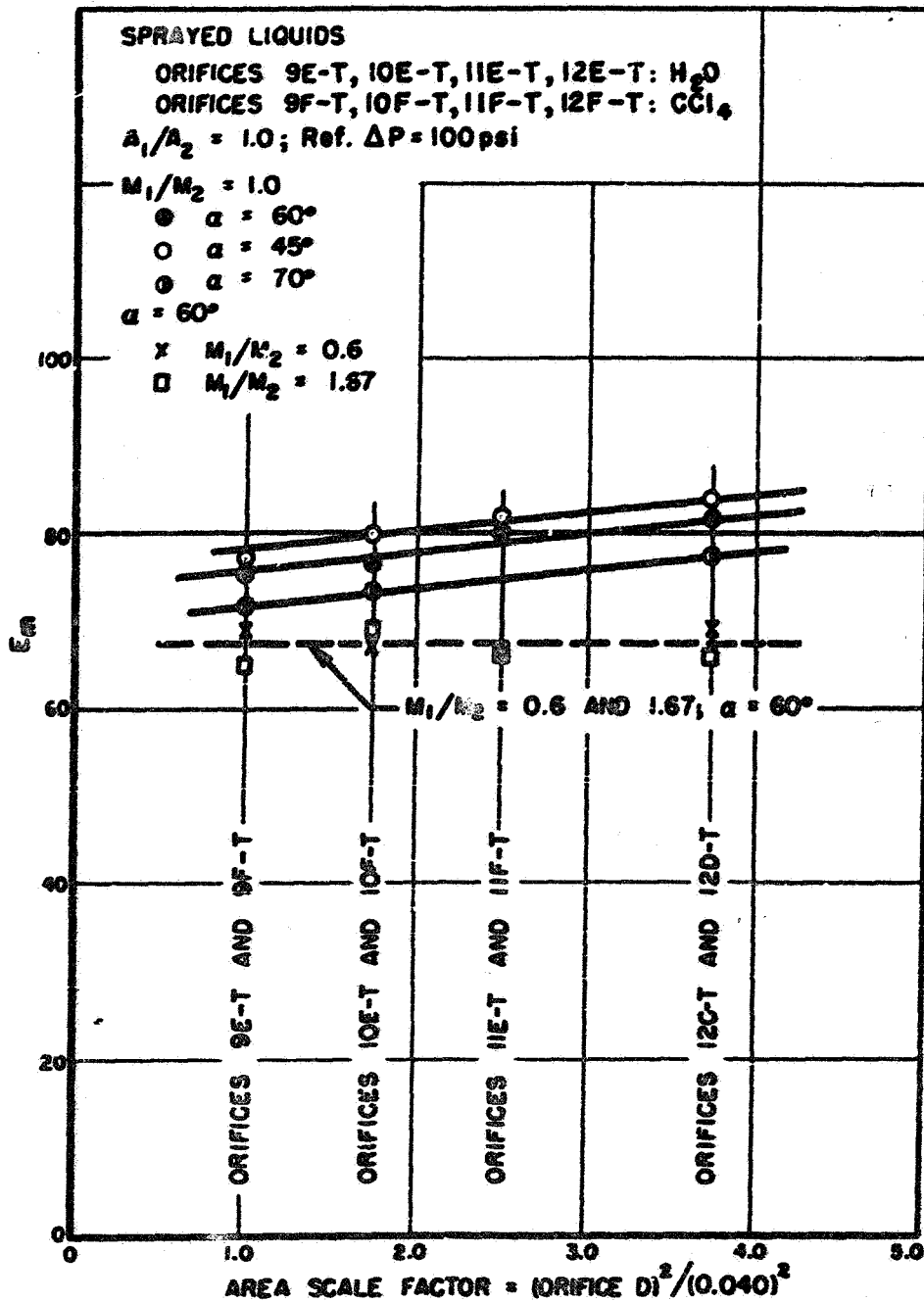
Figure 19.   Variation of E_m with Area Scale
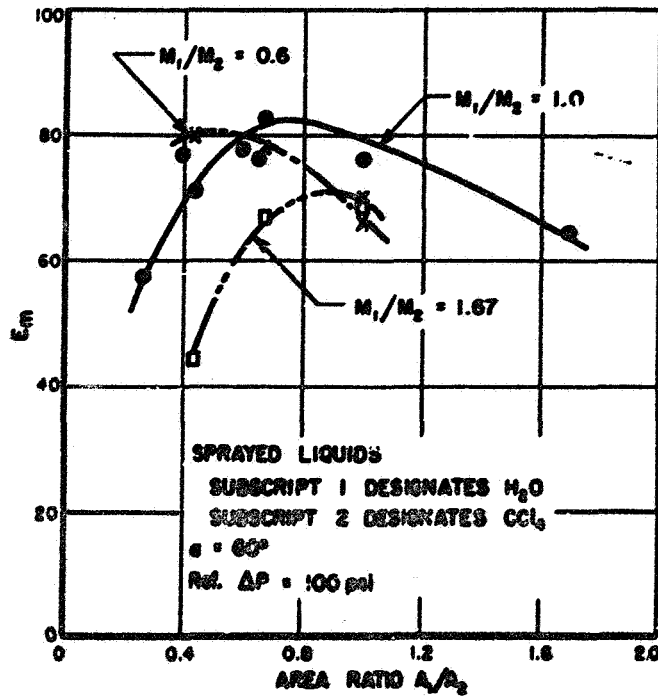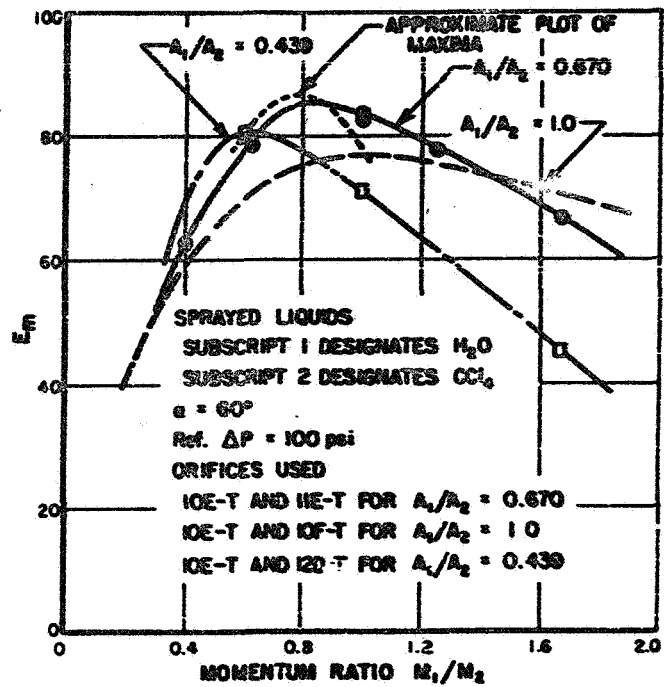
Figure 20

Variation of E_m with Area Ratio for Three Momentum Ratios

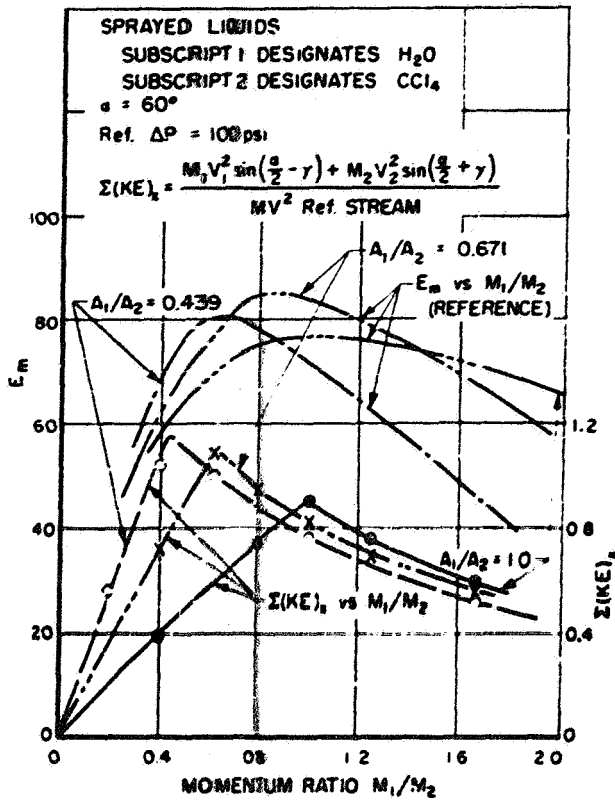Figure 21. Variation of E_m with Momentum Ratio for Three Area Ratios
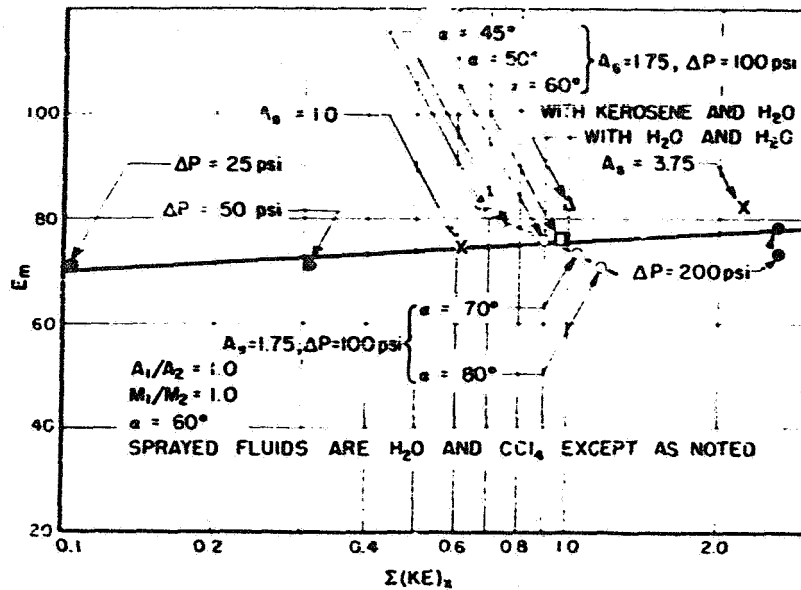
Figure 22

Kinetic Energy Available for Mixing

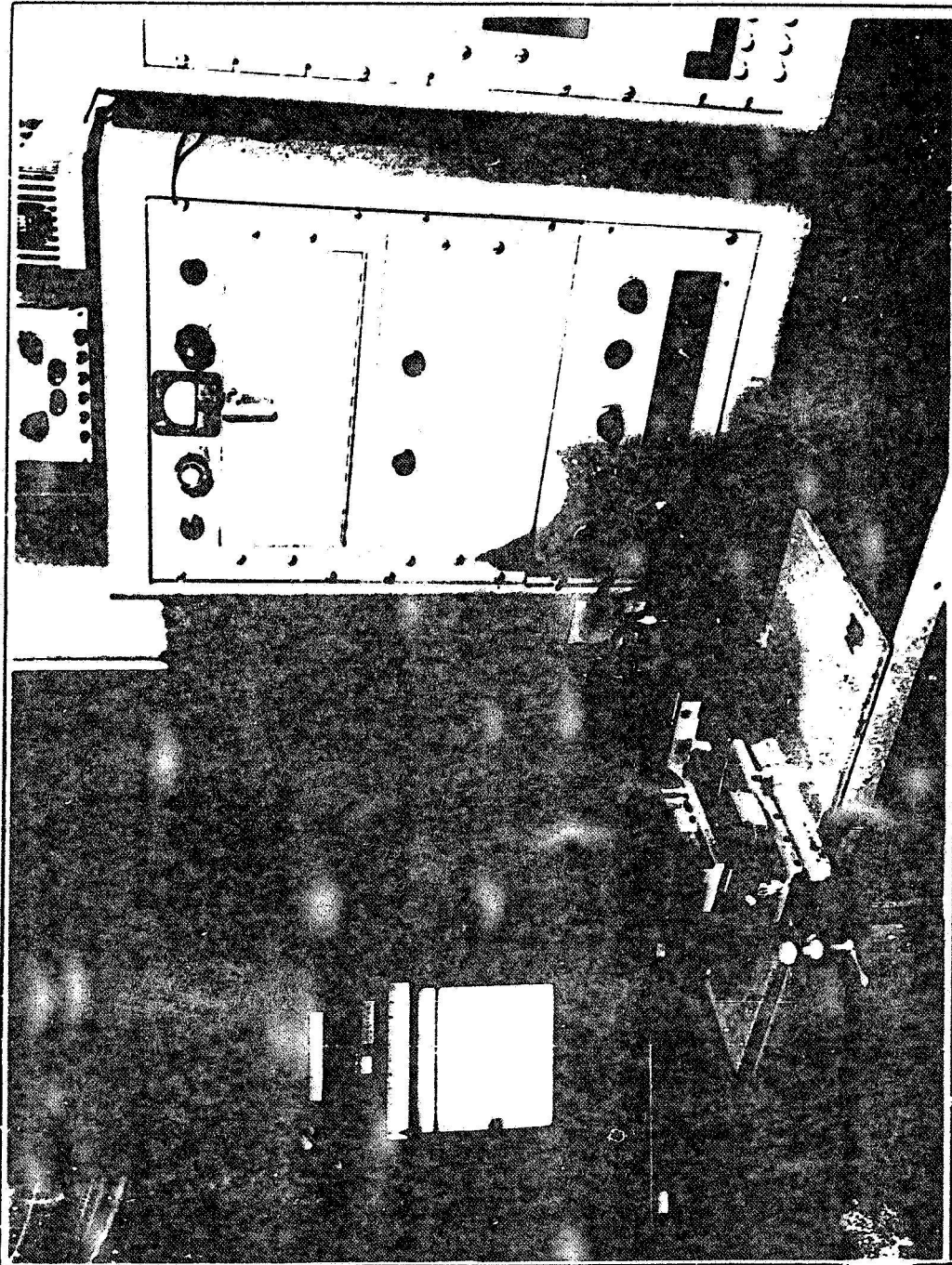Figure 23.   Variation of E_m with Energy Levels

Figure 24.   Photoelectric Densitometer

REFERENCES

1. Hausmann, H. K., and Nooggerath, W. C., *Design of Rocket-Motor Injectors for Use with Liquid Hypergolic Propellants*, NOTS 157. Inyokern (Calif.): U. S. Naval Ordnance Test Station, October 2, 1948 (Confidential).

2. Schwartz, A. M., and Perry, J. W., *Surface Active Agents, Their Chemistry and Technology*. New York: Interscience Publishers, 1949.

3. Kircher, H. J., and Mead, L., *Experimental and Theoretical Investigation of Rocket Engines to Determine Operating Characteristics of Various Design Parameters*, Report No. RMI-294-Q6. Rockaway (N. J.): Reaction Motors, July 25, 1950 (Restricted).

4. Weisenberg, I., et al, *Experimental and Theoretical Investigation of Rocket Engines to Determine Operating Characteristics of Various Design Parameters*, Report No. RMI-294-Q9. Rockaway (N. J.): Reaction Motors, January 15, 1951 (Restricted).

5. Freeman, J. R., "Experiments Relating to the Hydraulics of Fire Streams," *Transactions of the American Society of Civil Engineers*, 21:303-482, 1889.

6. Blair, J. S., "Characteristics of Fire Jets," *Journal of the Institution of Civil Engineers* (London), 16:354-360, 1940-1941.

7. Howe, J. W., and Posey, C. J., *Characteristics of High Velocity Jets*, Bulletin 21 of Studies in Engineering. Iowa City: University of Iowa, 1947.

8. Rouse, Hunter, and Hassan, M. M., "Cavitation Free Inlets and Contours," *Mechanical Engineering*, 71(No. 3):213-219, 1949.

9. Prandtl, L., and Tietjens, O. G., *Applied Hydro- and Aeromechanics*. New York: McGraw-Hill Book Company, 1934.

10. Rouse, Hunter, *Elementary Mechanics of Fluids*. New York: John Wiley and Sons, 1946.

11. Richardson, E. G., *Dynamics of Real Fluids*. London: Edward Arnold and Company, 1950.

12. Bakhmeteff, Boris A., *Mechanics of Turbulent Flow*. Princeton (N. J.): Princeton University Press, 1941.

13. Shapiro, Ascher H., and Smith, R. Douglas, *Friction Coefficients in the Inlet Length of Smooth Round Tubes*, Technical Note No. 1785. Washington: National Advisory Committee for Aeronautics, November, 1948.

REFERENCES (Cont'd)

14. Hagerty, R. P., and Jensen, F. G., *Investigation of a Rocket Burner and Observations on "Short Tube" Injection Orifices*, Technical Note No. RPD 51. London: Royal Aircraft Establishment, June, 1951 (Secret).

15. Hauschild, *Influence of the Position of the Efflux Borehole to the Axis of the Feed Channel and Also Influence of the Feed Channel Itself* (translated from German), Archiv 39/12 gK, March 25, 1942.

16. Northup, R. P., *An Experimental Investigation of the Flow and Stability of Liquid Streams from Small Orifices Discharging into a Gaseous Atmosphere*, Report No. R51A0512. Schenectady: General Electric Company, February, 1951 (Restricted).

17. Heidmann, Marcus F., and Humphrey, Jack C., *Fluctuations in a Spray Formed by Two Impinging Streams*, Technical Note No. 2349. Washington: National Advisory Committee for Aeronautics, April, 1951.

18. Elko, E. R., and Stary, M. L., *Final Report and Design Handbook of Acid-Aniline Rocket Motor and Injector Design*, Report No. 455. Azusa (Calif.): Aerojet Engineering Corporation, June 9, 1950 (Confidential).

19. *Handbook of Chemistry and Physics*, 25th ed. Cleveland (Ohio): Chemical Rubber Company, 1941.

THIS REPORT HAS BEEN DISTRIBUTED ACCORDING TO SECTIONS
A, C, AND DP OF THE COMMITTEE ON GUIDED MISSILES (R&D),
OFFICE OF THE SECRETARY OF DEFENSE, GUIDED MISSILE
TECHNICAL INFORMATION DISTRIBUTION LIST, MML 200/3, LIST
NO. 3, DATED 1 JULY, 1953 AND CHANGE SHEET NO. 1, DATED
26 OCTOBER, 1953.